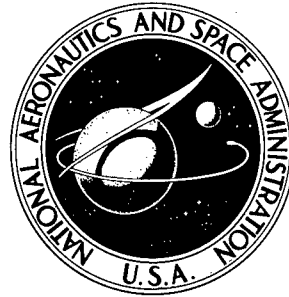


74287

P

NASA TECHNICAL NOTE

NASA TN D-5140



NASA TN D-5140

AMPTIAC

FACTORS INFLUENCING LOW-CYCLE CRACK
GROWTH IN 2014-T6 ALUMINUM SHEET
AT -320° F (77 K)

by William S. Pierce and Timothy L. Sullivan

Lewis Research Center

Cleveland, Ohio

Reproduced From
Best Available Copy

20000711 197

NATIONAL AERONAUTICS AND SPACE ADMINISTRATION • WASHINGTON, D. C. • APRIL 1969

DTIC QUALITY INSPECTED 4

NASA TN D-5140

FACTORS INFLUENCING LOW-CYCLE CRACK GROWTH IN 2014-T6
ALUMINUM SHEET AT -320° F (77 K)

By William S. Pierce and Timothy L. Sullivan

Lewis Research Center
Cleveland, Ohio

DISTRIBUTION STATEMENT A
Approved for Public Release
Distribution Unlimited

NATIONAL AERONAUTICS AND SPACE ADMINISTRATION

For sale by the Clearinghouse for Federal Scientific and Technical Information
Springfield, Virginia 22151 - CFSTI price ~~\$9.00~~

ABSTRACT

An investigation was conducted to determine the low-cycle (under 10 000 cycles) crack growth characteristics of through-center-cracked specimens 0.060 in. (0.152 cm) thick subjected to tension-tension cyclic loading. The following factors were studied: (1) minimum to maximum initial stress intensity ratio R_i ; (2) the maximum gross stress applied, as percentage of critical fracture stress; and (3) cyclic rate. The crack growth rate was found to be a function of stress level expressed as percentage of critical fracture stress for specimens tested at the same R_i value. A crack growth relation was developed which takes into account changes in R_i in the low-cycle region. When the cycle rate was decreased from 0.5 to 0.05 Hz, the cyclic life was reduced, but only for high initial stress intensities.



FACTORS INFLUENCING LOW-CYCLE CRACK GROWTH IN 2014-T6

ALUMINUM SHEET AT -320° F (77 K)

by William S. Pierce and Timothy L. Sullivan

Lewis Research Center

SUMMARY

An investigation was conducted to determine the low-cycle (under 10 000 cycles) crack growth characteristics of through-center-cracked 2014-T6 aluminum specimens 0.060 inch (0.152 cm) thick subjected to tension-tension cyclic loading at -320° F (77 K). The following factors were studied: (1) initial stress intensity ratio, varying from 0 to 0.7; (2) the maximum gross stress applied, as percentage of critical fracture stress varying from 60 to 90 percent; and (3) the cyclic rate ranging from 0.05 to 0.5 hertz.

The crack growth rate da/dN is a function of the percentage of critical fracture stress for specimens tested at the same ratio of minimum to maximum initial stress intensity. As was expected for these cases, the growth rate increased with an increase in the percentage of critical fracture stress (for equal values of crack length, $2a$).

A crack growth relation was developed which takes into account changes in the ratio of minimum to maximum initial stress intensity in the low-cycle region.

When the cycle rate was decreased from 0.5 to 0.05 hertz, the cyclic life was halved at a ratio of maximum initial stress intensity to nominal fracture toughness equal to 0.9. As this ratio was decreased to 0.6, the effect of cyclic rate on cyclic life became negligible.

INTRODUCTION

Structures such as cryogenic propellant tanks may undergo many cycles of loading during their lifetime. Such cyclically loaded structures may be subjected to fatigue crack growth during a portion of their lives because of the presence of material defects. Therefore, in recent years considerable effort has been expended to determine the factors which influence cyclic crack growth and to develop cyclic crack growth equations which take these factors into account. Knowledge of the effects of these factors will help to

prevent premature failure of cyclically loaded structures.

Paris (ref. 1) developed a power law relation for crack growth rate as a function of stress intensity factor range. Broek and Schijve (ref. 2) modified the Paris relation to account for the effects of change in R_i (the ratio of minimum to maximum initial stress intensity factors $K_{\min,i}/K_{\max,i}$) and the effect of specimen width. Forman (ref. 3) also modified Paris' relation to account for changes in R_i and to meet certain end-point conditions. Hudson and Scardina (ref. 4) compared the relations developed in references 1 to 3, with Forman's equation giving the best fit to the data. However, all these investigators have fit their equations to data which have cyclic lives in excess of 10 000 cycles. In reference 5 it was found that, for the low-cycle region, Forman's equation did not adequately account for the effects of change in R_i . Therefore, a modification to Forman's work is proposed in this report to account for changes in R_i in the low-cycle area.

Because little information is available on crack growth rates in the low-cycle region, a research program was conducted at the Lewis Research Center to determine the effects of various factors on the crack growth rate and cyclic lives in the crack growth life region under 10 000 cycles. The material chosen for this investigation was the aluminum alloy 2014-T6, which is currently being used in several launch vehicle systems. In these systems, the material may be subjected to cryogenic temperature. Therefore, the tests were conducted at -320°F (77 K), where this material is more sensitive to the presence of flaws or cracks (ref. 6).

This report presents the results of tests to determine the crack growth characteristics of through-center-cracked specimens 0.060 inch (0.152 cm) thick subjected to tension-tension cyclic loading. The following factors which affect cyclic crack growth rate were experimentally investigated: (1) initial stress intensity ratio, R_i ; (2) the maximum gross stress applied, as percentage of critical fracture stress; and (3) the cyclic rate. The value of R_i was varied from 0 to 0.7, percentage of critical fracture stress from 60 to 90, and cyclic rate from 0.05 to 0.5 hertz. Also a crack growth rate relation which accounts for changes in R_i is presented for the low-cycle crack growth region. The effect of R_i on cyclic life and scatter bands for groups of identical tests are also presented.

SYMBOLS

- a half-crack length, in. ; cm
- \bar{a} half-crack length corrected for plasticity effects, in. ; cm
- C coefficient (eqs. (6) and (7))
- C_1 coefficient (eq. (5))

C_2	coefficient (eq. (10))
E	modulus of elasticity, psi; gN/m^2
f	frequency, Hz
g	constant (eqs. (3) and (4))
h	constant (eq. (3))
K	stress intensity factor, $\text{ksi}\sqrt{\text{in.}}$; $\text{MN/m}^{3/2}$
ΔK	stress intensity factor range, $K_{\text{max}} - K_{\text{min}}$, $\text{ksi}\sqrt{\text{in.}}$; $\text{MN/m}^{3/2}$
K_{cc}	cyclic critical stress intensity factor, $\text{ksi}\sqrt{\text{in.}}$; $\text{MN/m}^{3/2}$
K_{cn}	nominal fracture toughness, $\text{ksi}\sqrt{\text{in.}}$; $\text{MN/m}^{3/2}$
m	exponent (eqs. (5) and (10))
N	number of load cycles
R	ratio of $K_{\text{min}}/K_{\text{max}}$ in a given cycle (positive stress only)
W	sheet width, in.; cm
α, β	constants (eq. (7))
γ	exponent (eq. (6))
δ, θ	constants (eq. (8))
σ	uniform gross fracture stress acting normal to plane of crack, ksi; MN/m^2
σ_{ys}	uniaxial yield strength, ksi; MN/m^2

Subscripts:

c	critical
f	failure
i	initial condition (first cycle)
l	last complete cycle before failure
max	value at maximum cyclic load
min	value at minimum cyclic load

APPARATUS AND PROCEDURE

Specimens were machined from sheet nominally 0.060 inch (0.152 cm) thick. All material came from a single heat of 2014-T6 aluminum. Its chemical composition is given in the following table:

Aluminum alloy composition, wt. %							
Cu	Si	Mn	Mg	Fe	Zn	Cr	Ti
4.45	0.92	0.69	0.57	0.60	0.05	0.04	0.02

Crack Growth Specimens and Test Procedure

For the cyclic crack growth studies, 3-inch- (7.6-cm-) wide center-cracked specimens were used. Specimens were machined so that the center crack was normal to the sheet rolling direction. The center crack for all the tests was approximately 0.3 inch (0.8 cm) long. Complete dimensions of this specimen are given in figure 1(a). The tests were conducted at -320°F (77 K) by immersing the specimens in liquid nitrogen.

Continuity gages (ref. 7) were used to measure cyclic crack growth. Calibration tests showed that the gages gave an accurate indication of the crack length. An instru-

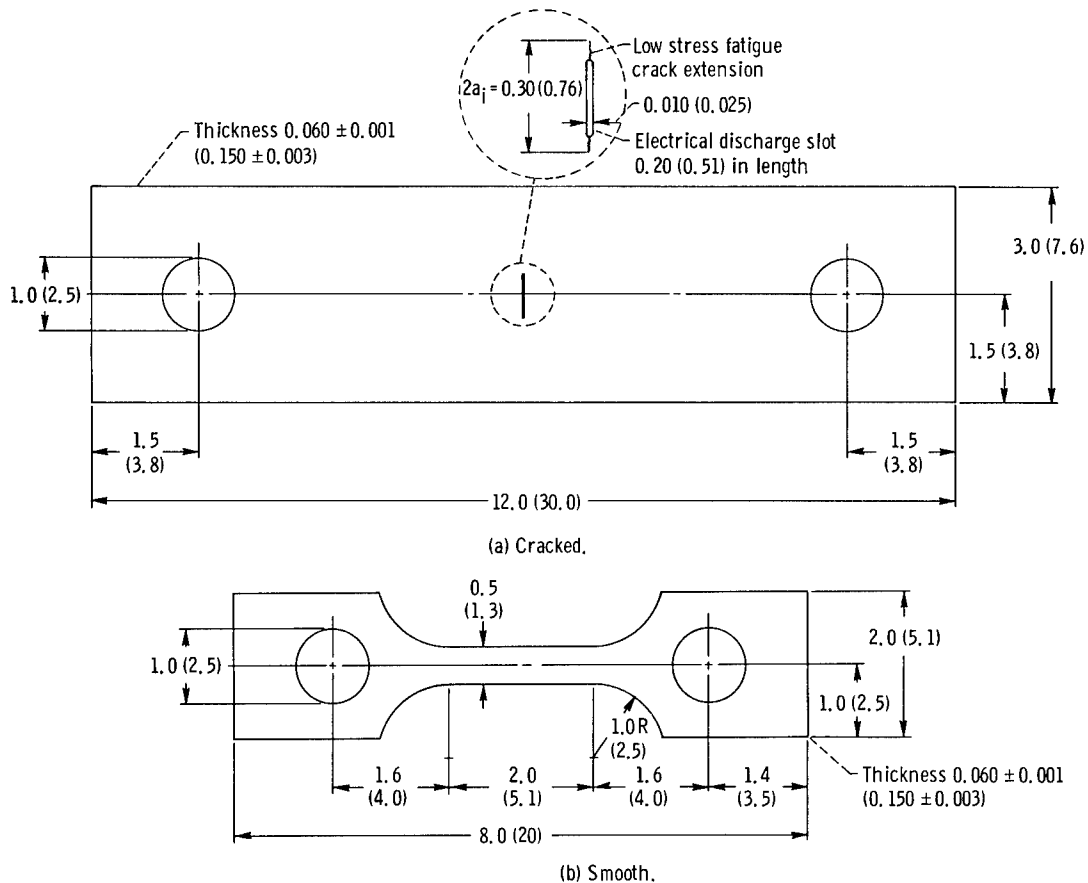
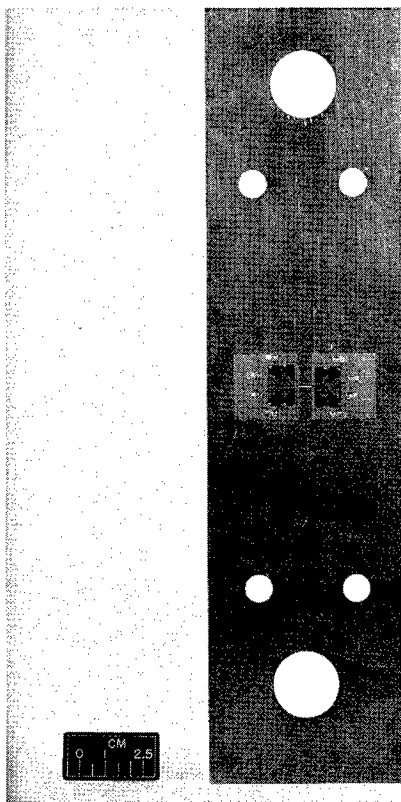
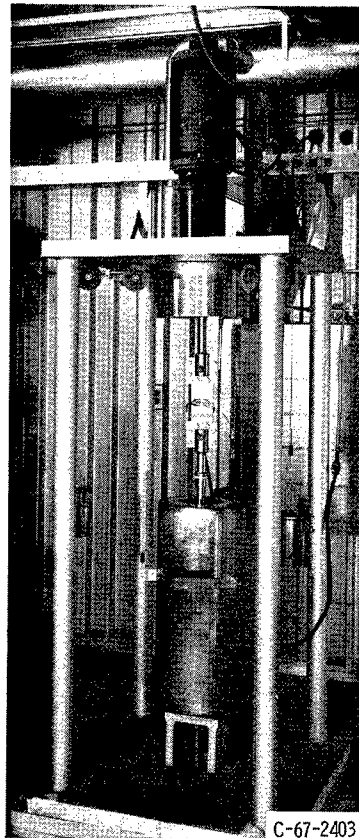


Figure 1. - Smooth and cracked tensile specimens. (Dimensions are in inches (cm).)



C-68-2972

Figure 2. - Cracked tensile specimen with continuity gages.



C-67-2403

Figure 3. - Specimen installed in tensile fatigue testing machine with cryostat in lowered position.

mented specimen is shown in figure 2. Load and continuity gage output were recorded on a multichannel direct-recording oscillograph. From the oscillograph trace, the crack length after each cycle could be determined within ± 0.01 inch (± 0.03 cm).

The fatigue machine used in this study is shown in figure 3. A servocontrolled closed-loop load control system was used. A hydraulic cylinder provided load and was controlled by an electrohydraulic servovalve. A dual-bridge strain-gage load transducer provided the control system feedback signal and the oscillograph load readout signal. A function generator provided a sinusoidal command signal. The fatigue machine was capable of applying a maximum load of 20 000 pounds (89 000 N). Its limiting frequency was about 1 hertz.

After the test specimen was inserted in the machine, the cryostat was raised to surround the specimen. The cryostat was then filled with liquid nitrogen. Liquid level was monitored with carbon resistor probes. Additional liquid was added as required during the test to keep the specimen totally immersed.

Material Property Tests

The static material properties at room and cryogenic temperatures were obtained from Orange (ref. 6). The same heat and thickness of material used by Orange was used in this study. The type of specimen used to determine the 0.2 percent offset yield strength, ultimate strength, and elastic modulus is shown in figure 1(b). The test results are given in table I.

ANALYSIS

Stress Intensity Calculations

Calculation of the stress intensity in a finite-width center-cracked sheet subjected to uniform tension requires a correction for width effect. The Irwin-Westergaard tangent relation has been commonly used for width effect correction. Paris and Sih (ref. 8) indicate that a more accurate width correction is available from the work of Isida (ref. 9). In the discussion portion of reference 10, C. E. Feddersen points out that the polynomial correction of Isida can be replaced with a very compact secant expression. For ratios of crack length to specimen width $2a/W$ up to 0.8, the secant expression approximates the Isida polynomial within 0.3 percent.

The stress intensities and fracture toughness values reported herein were calculated by using the secant width correction expression as indicated in the following equation:

$$K = \sigma \sqrt{\pi \bar{a} \sec \frac{\pi \bar{a}}{W}} \quad (1)$$

In equation (1) the half-crack length is corrected for plasticity effects by

$$\bar{a} = a + \frac{1}{2\pi} \frac{K^2}{\sigma_{ys}^2}$$

Nominal fracture toughness K_{cn} can be calculated from the initial half-crack length a_i by using the equation

$$K_{cn} = \sigma_c \sqrt{\pi \bar{a}_i \sec \frac{\pi \bar{a}_i}{W}} \quad (2)$$

where

$$\bar{a}_i = a_i + \frac{1}{2\pi} \frac{K_{cn}^2}{\sigma_{ys}^2}$$

Nominal fracture toughness K_{cn} is always equal to or less than the critical stress intensity (fracture toughness) K_c . For cases where subcritical crack growth is only a small percentage of the initial crack length, K_{cn} is a reasonable approximation of K_c .

The value of K_c reported in table I was obtained from the data in reference 6. However, the secant width correction (eq. (1)), rather than the tangent correction, was used in the calculations. The value reported is based on data from wider specimens than were used in this study.

The value of K_{cn} was also obtained by using the secant width correction (eq. (2)). Data for 3-inch- (7.6-cm-) wide specimens were taken from reference 6. Because specimens with 0.3-inch (0.76-cm) cracks were not tested in reference 6, it was necessary to interpolate between results obtained from specimens with 1/4- and 1/2-inch (0.64- and 1.27-cm) cracks. The value for σ_c was also obtained by interpolation.

Growth Rate Calculations

Two methods were used to determine $d(2a)/dN$ as explained in the following paragraphs. It was originally planned that only one method, which used a computer, would be used for the entire program. However, as explained below, under certain conditions meaningful values could not be obtained with this approach. Therefore, the more-time-consuming hand calculations were used when the computer method did not give accurate values of $d(2a)/dN$. Figure 4 shows a comparison of the growth rate curves obtained by both methods.

For specimens 1 to 24, which were used for the data presented in figures 8 to 11 and figure 14 (pp. 13 to 17, and p. 20), the following method was used to calculate the crack growth rate da/dN . Data showing the crack length as a function of number of stress cycles were plotted, and a smooth curve was drawn to give a good visual fit. Figure 5(a) is typical of the curves obtained. Ten points were selected on each curve. At each point the slope $d(2a)/dN$ was determined graphically and instantaneous values of K_{max} and K_{min} were calculated by using equation (1). The same value of a was used to calculate both K_{max} and K_{min} . (Conditions in which compressive stresses are involved were not examined and are not part of this study.) In figures 8 to 11 and 14 the growth rate is plotted as da/dN . The calculated values and test conditions are presented in tables II and III for specimens 1 to 24.

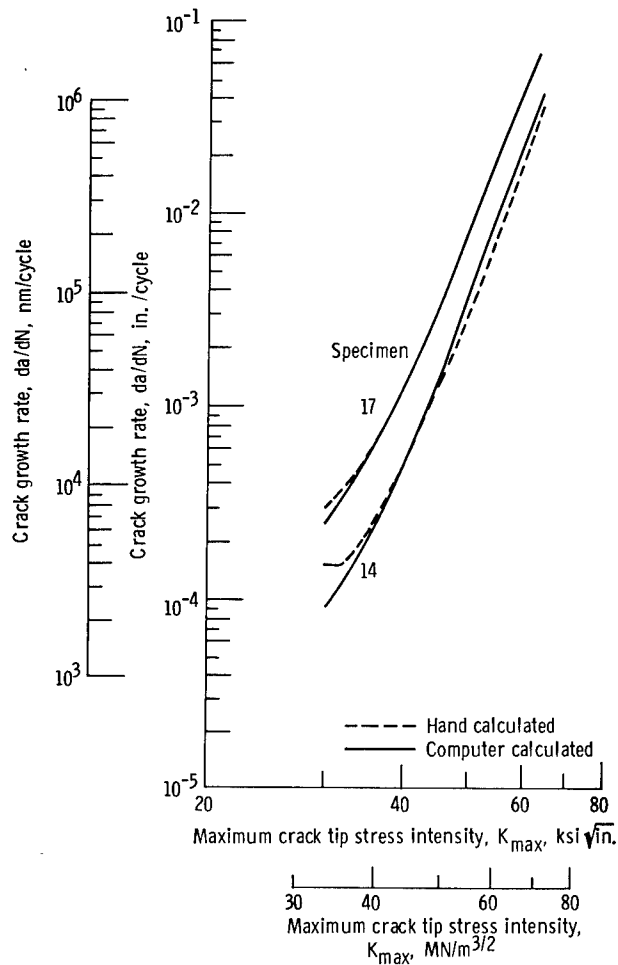


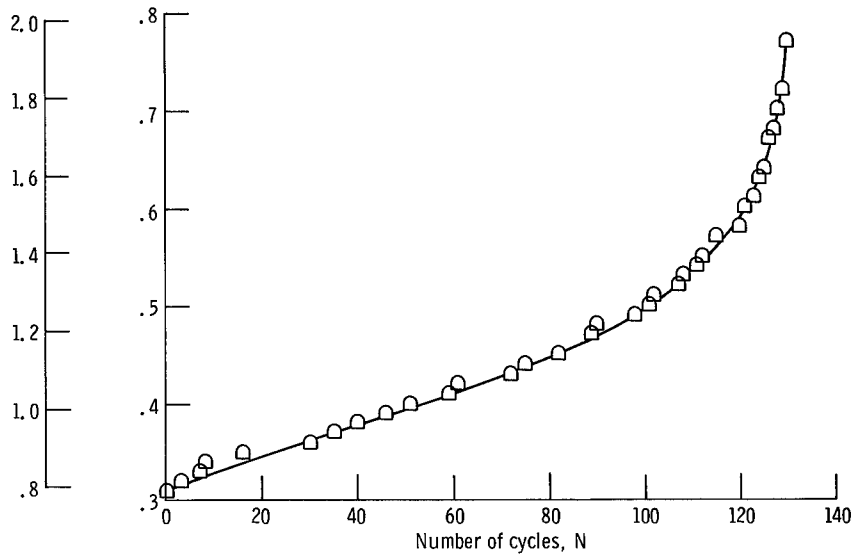
Figure 4. - Comparison of crack growth rates obtained from hand-calculated and computer-calculated slopes.

For specimens 25 to 54, which were used for the data presented in figures 12 and 13, the following method was used to calculate the crack growth rates. The data were plotted as crack length versus \log_e of the number of cycles remaining $N_f - N$. Figure 5(b) is typical of the curves obtained. A least-squares fit was used to determine the equation of the curve in figure 5(b). This equation was assumed to have the following general form:

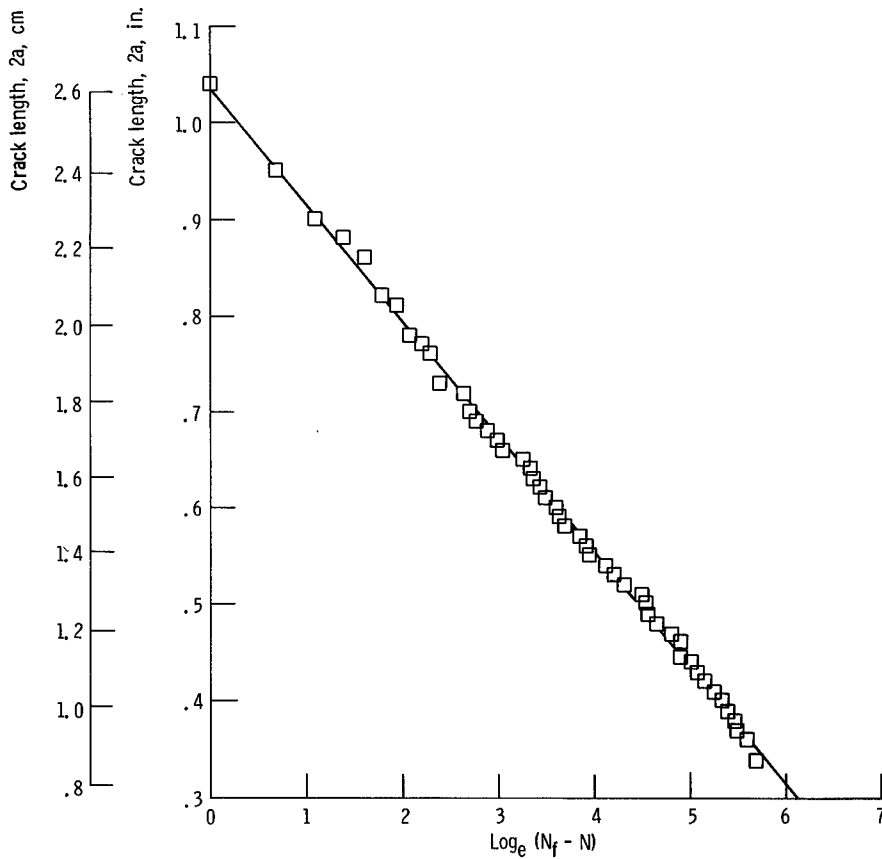
$$2a = g \log_e(N_f - N) + h \quad (3)$$

Differentiation of equation (3) gives the following relation for crack growth rate:

$$\frac{d(2a)}{dN} = \frac{g}{N_f - N} \quad (4)$$



(a) Crack length as function of stress cycles. Specimen 6.



(b) Crack length as function of stress cycles remaining. Specimen 40. Crack length, $2a = g \log_e(N_f - N) + h$.

Figure 5. - Typical crack growth curves for 2014-T6 aluminum at -320°F (77 K).

Ten representative points were selected on each curve. At each point the crack growth rate was calculated by using equation (4). Values for K_{\max} and K_{\min} were calculated by using equation (1), as in the previous method. The calculated values and test conditions are presented in tables II and IV for specimens 25 to 54.

It was found that equation (3) gave a good fit with the experimental data up to a life of about 1500 cycles. For longer lives the experimental data deviated from equation (3) by an amount too large to get accurate values of $d(2a)/dN$ from equation (4). Specimens 1 to 24 were used to determine the effect of R_i on da/dN . Some of these specimens had lives as long as 8600 cycles. For consistency, da/dN for all these specimens regardless of cyclic life was determined graphically. Specimens 25 to 54 were used to investigate scatter and the effect of cyclic rate on life and da/dN . All these specimens failed in less than 1560 cycles; hence, equation (4) was used to obtain da/dN .

Crack Growth Rate Equation

As described in the INTRODUCTION, Forman's equation (ref. 3) gave good agreement with data in which the cyclic life was primarily above 10 000 cycles. In reference 5 and in this investigation it was found that for the low-cycle crack growth region, Forman's equation did not adequately account for the effects of change in R_i . Also, it was found in reference 5 that the slope of the growth rate curve appeared to be a function of R_i . Therefore, Forman's equation

$$\frac{da}{dN} = \frac{C_1 \Delta K^m}{(1 - R)K_c - \Delta K} \quad (5a)$$

which can be written as

$$\frac{da}{dN} = \frac{C_1 (1 - R)^{m-1} K_{\max}^m}{K_c - K_{\max}} \quad (5b)$$

was modified to let the effects of R_i be partly accounted for by varying the exponent in the equation. The proposed equation takes the following form:

$$\frac{da}{dN} = \frac{CK_{\max}^\gamma}{K_{cc} - K_{\max}} \quad (6)$$

where γ and C are functions of R_i .

In equation (6), as in equation (5b), the denominator forces the growth rate to infinity as K_{max} approaches the critical stress intensity. The term K_{cc} (cyclic critical stress intensity) was used rather than K_c because it appears that, by cycling, a critical stress intensity can be obtained that is slightly higher than the normal static K_c value. The value of K_{cc} was assumed to be the maximum value of K_{max} approached by the curves of figure 8. This value was found to be $69.0 \text{ ksi} \sqrt{\text{in.}}$ ($75.8 \text{ MN/m}^{3/2}$) (approximately 4 percent higher than K_c for this material at -320° F (77 K)).

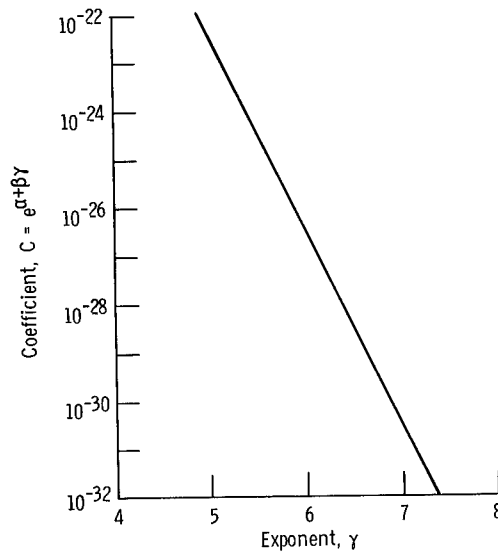


Figure 6. - Relation of coefficient C to exponent γ .

The constant C appears to be a straight-line function of γ when plotted on semilog coordinates (see fig. 6). This function can be written as

$$C = e^{\alpha + \beta\gamma} \quad (7)$$

The exponent γ was assumed to be a straight-line function of R_i , which takes the form

$$\gamma = \delta + \theta R_i \quad (8)$$

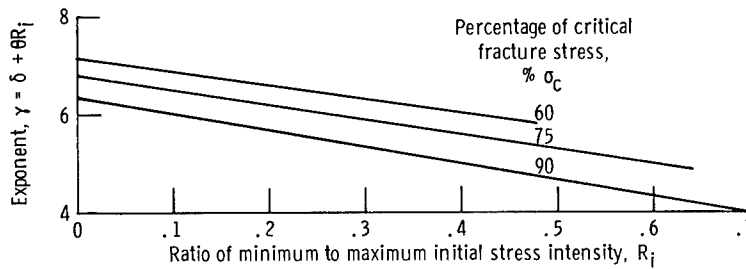


Figure 7. - Relation of γ to R_i ratio, for various percentages of critical fracture stress.

It was found that different values of δ and θ are required for each percentage of critical fracture stress. These results are plotted in figure 7.

RESULTS AND DISCUSSION

For all results except those associated with the cyclic rate and data scatter studies, two or three tests were made for each condition. The results were very similar, and therefore one specimen was selected out of each group to be used in the analysis and figures. Five identical specimens were run for the cyclic rate and scatter tests. The data are presented in tables III and IV for all specimens.

In the figures showing crack growth rates, some tests exhibited peculiar growth rates during the early stages of crack growth. This may be associated with establishing new conditions at the crack tip. This portion of the data was omitted from the figures but was included in the tables.

Effect of Percentage of Critical Fracture Stress on Crack Growth

In figures 8(a) to (c), crack growth rate is plotted as a function of maximum crack tip stress intensity for three percentages of critical fracture stress σ_c and various R_i ratios. These stress levels correspond to 60, 75, and 90 percent of the stress level required to cause fracture in a 3-inch- (7.6-cm-) wide specimen containing a 0.30-inch (0.76-cm) through-crack at -320° F (77 K). For equal R_i values and crack length, the crack growth rate increases with increase in percentage of critical fracture stress. This relation is shown by the dashed curve in figure 8(a) for $R_i = 0$. The same general trend appears in figures 8(b) and (c) for R_i of 0.23 and 0.47, respectively. Therefore, it appears that in discussing crack growth rate, we must consider not only maximum stress intensity and stress intensity ratio R_i , but also the percentage of critical fracture stress (or maximum cyclic stress).

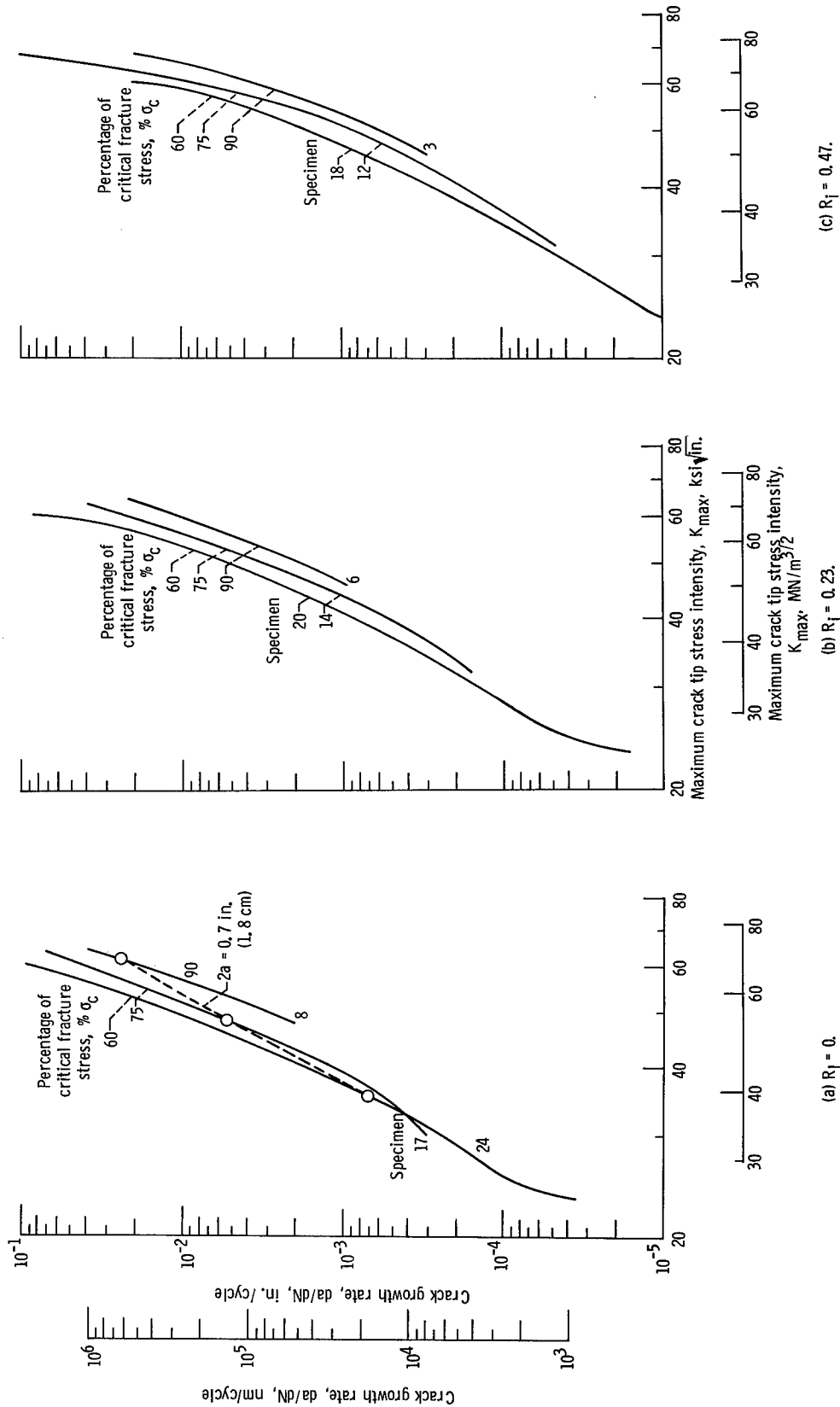


Figure 8. - Crack growth rate as function of maximum crack tip stress intensity for through-cracked tensile specimens for various percentages of critical fracture stress at a given ratio of minimum to maximum initial stress intensity (R_1 ratio).

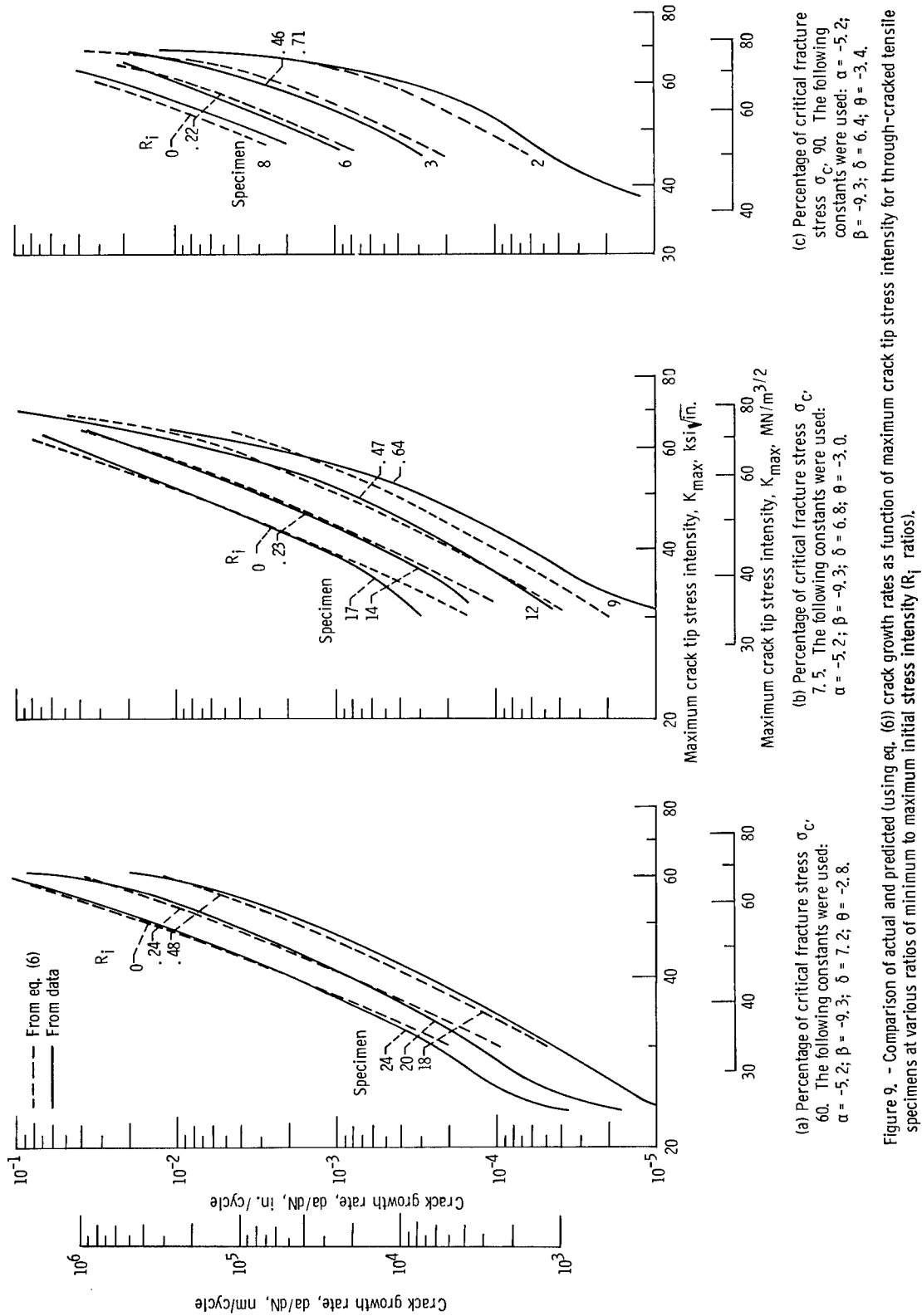


Figure 9. - Comparison of actual and predicted (using eq. (6)) crack growth rates as function of maximum crack tip stress intensity for through-cracked tensile specimens at various ratios of minimum to maximum initial stress intensity (R_i ratios).

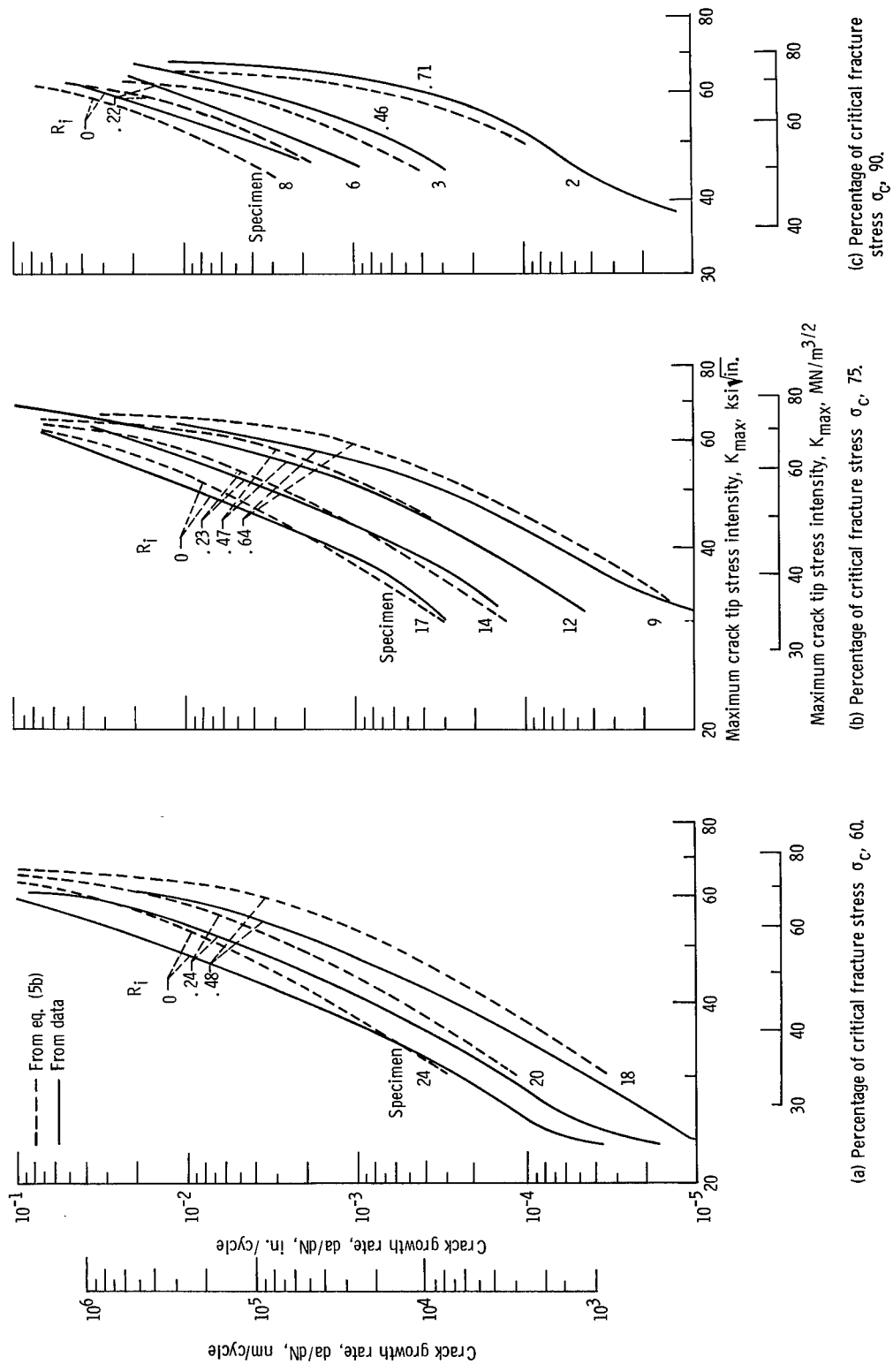


Figure 10. - Comparison of actual and predicted (using eq. (5b)) crack growth rates as function of maximum crack tip stress intensity for through-cracked tensile specimens at various ratios of minimum to maximum initial stress intensity (R_i ratios).

Crack Growth Relation

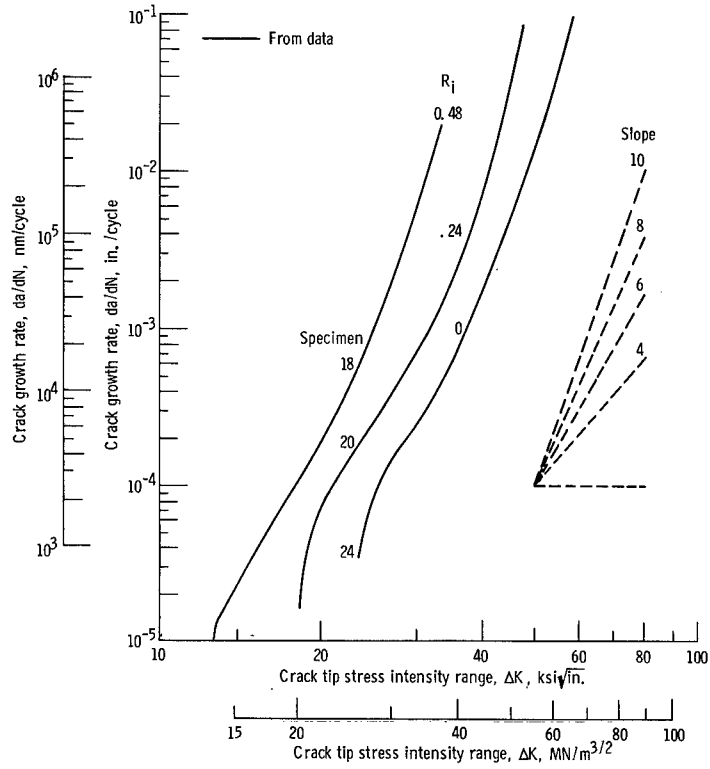
The crack growth relation presented in the section ANALYSIS (eq. (6)) is compared with the actual growth data in figures 9(a) to (c) for all test conditions. For each percentage of σ_c , a computer program was used to find the best values of α , β , δ , and θ to fit the data, considering all R_i ratios simultaneously. Once these values are known, C and γ can easily be calculated for any R_i ratio (positive stress only) by using equations (7) and (8). By running a minimum of one test specimen at each of two different R_i values (0 and 0.8) and the same percentage of σ_c , these factors (C and γ) could be determined without the use of a computer program. (The actual number of tests depends on the confidence level desired; see section Scatter Bands for Rate Tests.) By using a plot such as figure 9 and selecting two points on the curve for $R_i = 0$, a simultaneous solution of equation (6) will give one value of C and γ . Repeating this procedure for $R_i = 0.8$ will give another value for C and γ . Substitute these two values of C and γ into equation (7) and solve simultaneously for α and β . Similarly, substituting the values of γ and R_i into equation (8) gives values of δ and θ . With the values of α , β , δ , and θ determined, C and γ can be obtained for various R_i by using equations (7) and (8). The values of da/dN can then be calculated by using equation (6) and the appropriate values of C and γ .

This procedure would be valid for only one percentage of σ_c . As shown by the various curves in figure 7, δ and θ must be determined for each percentage of σ_c . Two more specimens would have to be tested for each desired percentage of σ_c .

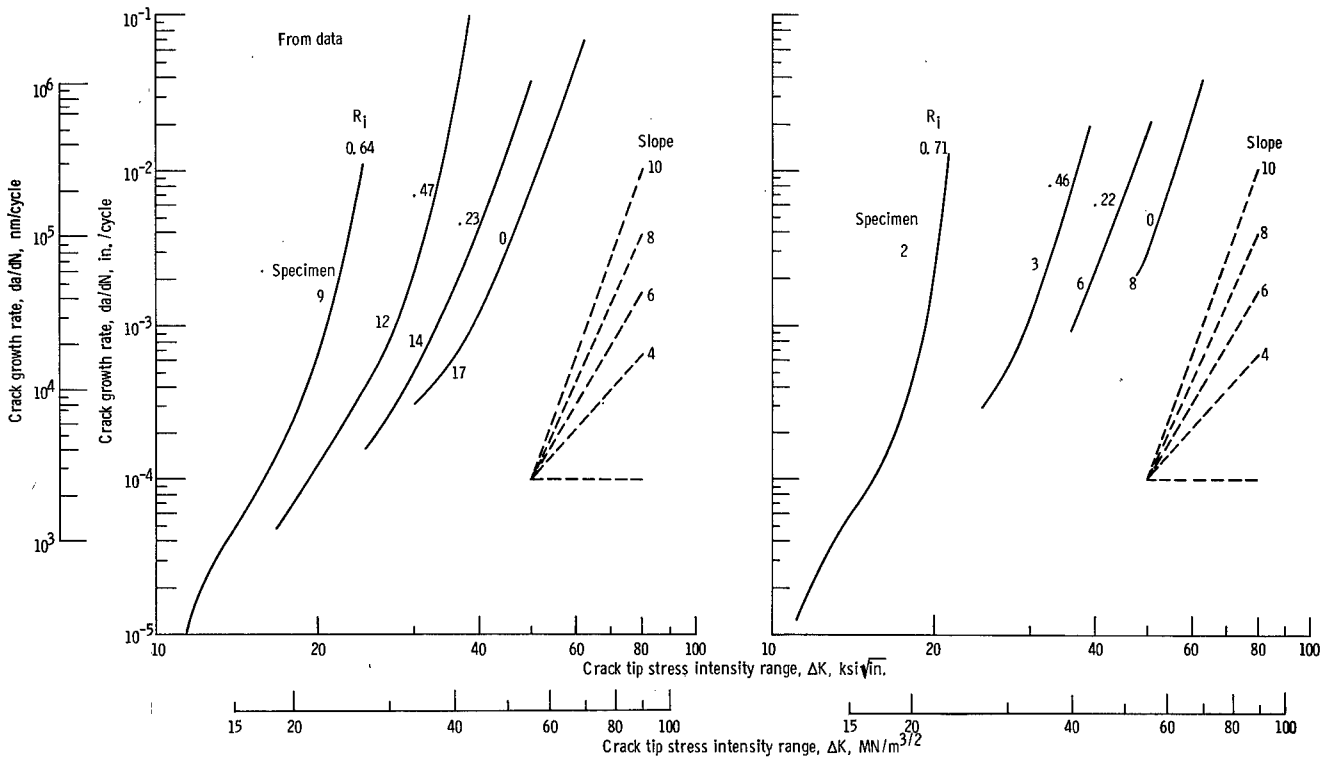
In figures 10(a) to (c) the crack growth rate curves obtained by using Forman's method (eq. (5b)) are compared with the actual growth rate data. The values of C_1 and m used in the equation were 2.3×10^{-19} and 4.4, respectively. These constants were determined by using a least-squares fit to the data. In almost all cases, the results found by using the method presented in this study (eq. (6)) show better agreement with the actual data than do the values obtained by using the Forman method (eq. (5b)). However, if the constants in Forman's method were evaluated for each percentage of σ_c , a better fit than that shown in figure 10 would probably be obtained.

Effect of R_i Ratio on Crack Growth Rate

Figures 11(a) to (c) show crack growth rate da/dN as a function of crack tip stress intensity range ΔK for various R_i ratios at given percentages of critical fracture stress. In general, the slopes of the growth rate curves increase with increase in R_i . In all tests, the average slope of the curves is higher than 4 to 1. This slope corre-



(a) Percentage of critical fracture stress σ_c , 60.



(b) Percentage of critical fracture stress σ_c , 75.

(c) Percentage of critical fracture stress σ_c , 90.

Figure 11. - Crack growth rate as function of crack tip stress intensity range for through-cracked tensile specimens for various ratios of minimum to maximum initial stress intensity (R_i ratios) at given percentage of critical fracture stress.

sponds to the value of the exponent m in the Paris crack growth relation (ref. 1 and eq. (10))

$$\frac{da}{dN} = C_2 \Delta K^m \tag{10}$$

and usually appears in the literature as 4. In most of the results reported herein, the slope is more than double this value. A straight-line fit to the curve does not have much meaning because the slope varies considerably from one portion of the curve to another. Equation (5a) predicts a curve shape with increasing slope, such as that shown in figure 11. However, the predicted change in slope with change in R_i is not always great enough for the low-cycle tests of this study.

Effect of Cycle Rate on Growth and Life

The effect of cyclic rate on cycles to failure is shown in figure 12. When the cycle rate was reduced from 0.5 to 0.05 hertz, the cyclic life was decreased by almost one-

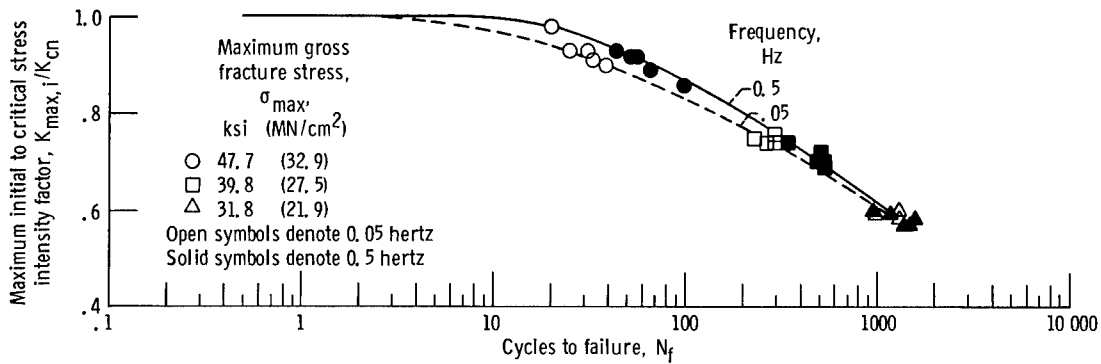
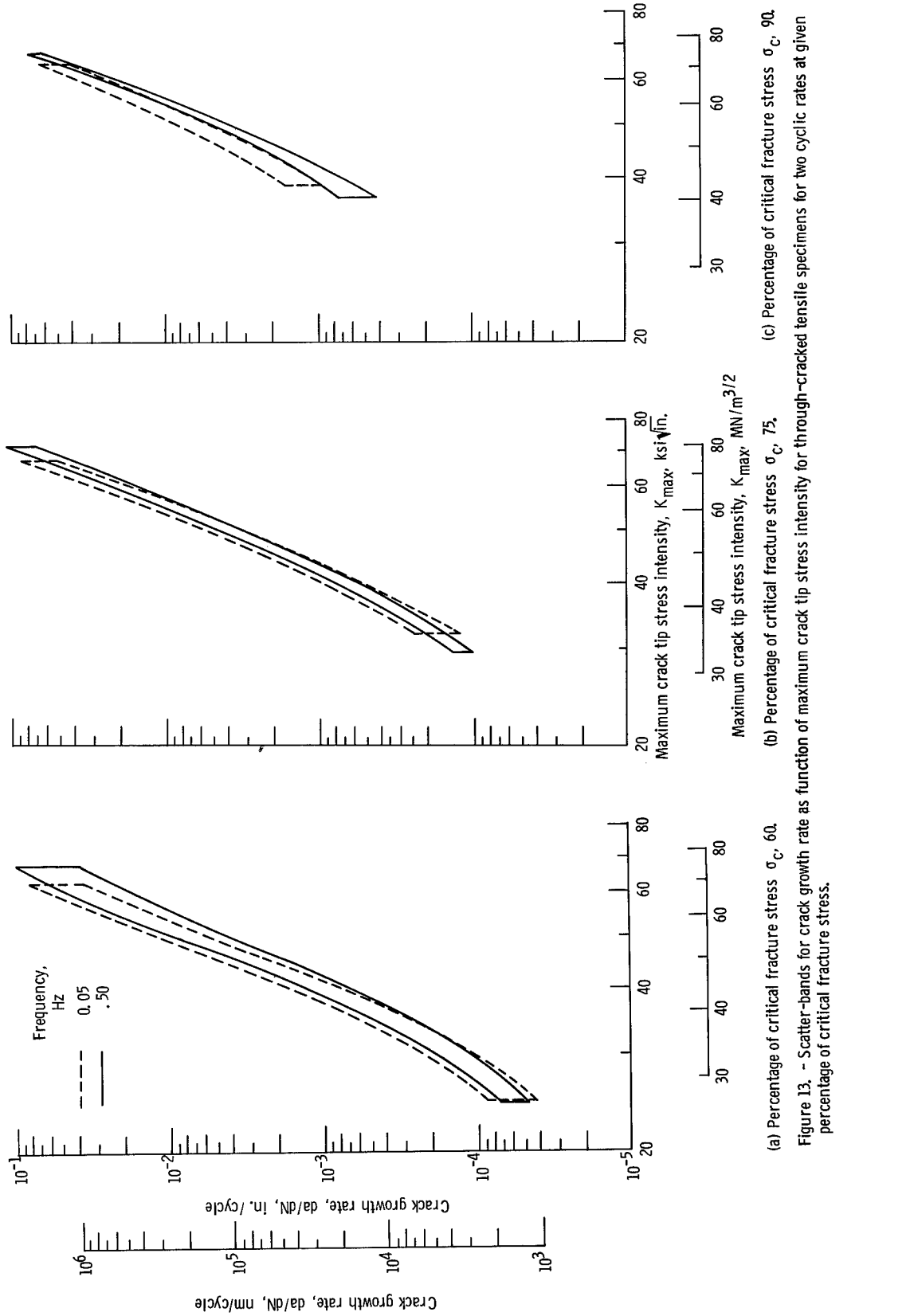


Figure 12. - Effect of ratio of maximum initial to nominal critical stress intensity $K_{max,i}/K_{cn}$ and cyclic rate on cycles to failure. Ratio of minimum to maximum initial stress intensity, $R_i = 0.1$.

half at $K_{max,i}/K_{cn} = 0.9$. As this ratio was decreased to about 0.6, the effect of cyclic rate on cyclic life became negligible.

The effect of cyclic rate on crack growth rate is shown in figures 13(a) to (c) for given percentages of critical fracture stress σ_c . The bands produced by the groups of five specimens are shown. In figures 13(a) and (b) (60 and 75 percent of σ_c) the bands produced for the two cyclic rates nearly coincide. At 90 percent of σ_c (fig. 13(c)) the bands are distinct, with the crack growth rate lower for specimens tested at 0.5 hertz than for those tested at 0.05 hertz. Thus, the change in crack growth rate and cyclic



(a) Percentage of critical fracture stress σ_c , 60.
 (b) Percentage of critical fracture stress σ_c , 75.
 (c) Percentage of critical fracture stress σ_c , 90.

Figure 13. - Scatter-bands for crack growth rate as function of maximum crack tip stress intensity for through-cracked tensile specimens for two cyclic rates at given percentage of critical fracture stress.

life due to cyclic rate is most predominant at high percentages of σ_c . This may be due to a time-dependent crack growth process which is most pronounced when the specimen is subjected to high stress levels.

Effect of Stress Intensity on Cycles to Failure

The effect of maximum stress intensity and stress intensity ratio on cycles to failure is shown in figure 14. A family of curves was drawn with one distinct curve for each R_i

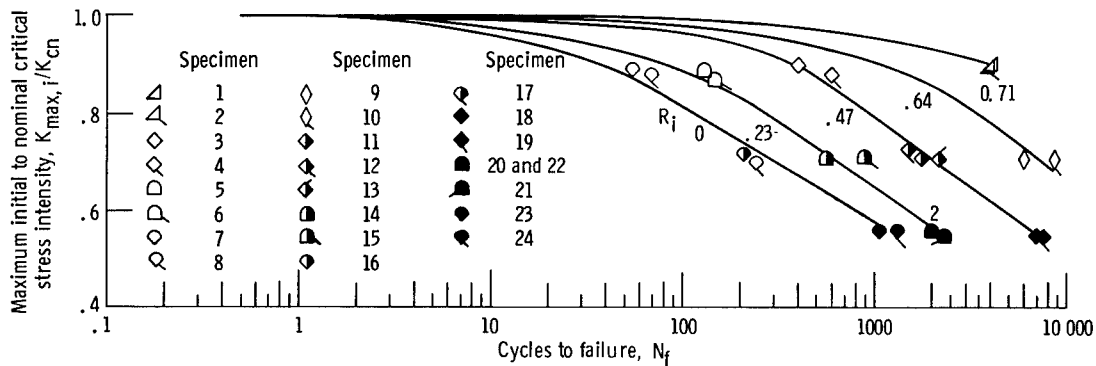


Figure 14. - Effect of ratio of maximum initial to nominal critical stress intensity $K_{max,i}/K_{cn}$ and ratio of minimum to maximum initial stress intensity (R_i ratio) on cycles to failure. See table 111 for initial specimen conditions and test data.

ratio. For a given value of $K_{max,i}/K_{cn}$, the cyclic life increases with increasing R_i or, conversely, the cyclic life decreases with increasing ΔK . For $K_{max,i}/K_{cn} = 0.7$, increasing R_i from 0 to 0.5 changed the cyclic life from 300 to 2100 cycles.

Scatter Bands for Rate Tests

The five duplicate specimens used to determine the effect of cyclic rate in figure 13 were also used to determine the approximate size of the data scatter band. These groups of five specimens were tested at three different percentages of σ_c and two cyclic rates. The maximum band width covered a growth rate range of about 2.5 to 1, as shown in figure 13(a) at 0.5 hertz.

SUMMARY OF RESULTS

An investigation was conducted to determine the low-cycle (less than 10 000 cycles) crack growth behavior and cyclic life at -320° F (77 K) of 2014-T6 aluminum through-cracked tensile specimens. The results are as follows:

1. The crack growth rate da/dN is a function of the percentage of critical fracture stress σ_c for specimens tested at the same R_i value (the ratio of minimum to maximum initial stress intensity factors $K_{\min,i}/K_{\max,i}$). When crack growth rate was plotted as a function of K_{\max} for various percentages of σ_c and constant R_i , the growth rate increased with increasing percentages of σ_c (for equal values of crack length $2a$).

2. A crack growth relation is presented which takes into account changes in R_i ratio (positive stress only) in the low-cycle region. The equation takes the following form:

$$\frac{da}{dN} = \frac{CK_{\max}^{\gamma}}{K_{cc} - K_{\max}}$$

where γ and C are functions of R_i and the percentage of critical fracture stress, N is the number of load cycles, and K_{cc} is the cyclic critical stress intensity factor.

3. For the cyclic lives studied, a log-log plot of crack growth rate against ΔK shows that the average slope of the growth rate curve increased with increase in R_i . The average slope of the curves was higher than 4 (a value used by Paris for data in the 10^4 - to 10^6 -cycle region) and in most cases was more than double this value.

4. When the cycle rate was reduced from 0.5 to 0.05 hertz, the cyclic life was decreased by almost one-half at a value of $K_{\max,i}/K_{cn} = 0.9$ (where K_{cn} is nominal fracture toughness). As this ratio was decreased to about 0.6, the effect of cyclic rate on cyclic life became negligible. The crack growth rate was lower for specimens tested at 0.5 hertz than for those tested at 0.05 hertz ($K_{\max,i}/K_{cn} = 0.9$).

Lewis Research Center,
National Aeronautics and Space Administration,
Cleveland, Ohio, December 18, 1968,
124-08-08-20-22.

REFERENCES

1. Paris, Paul C.: The Fracture Mechanics Approach to Fatigue. Fatigue - An Interdisciplinary Approach. John J. Burke, Norman L. Reed, and Volker Weiss, eds., Syracuse Univ. Press, 1964, pp. 107-132.
2. Broek, D.; and Schijve, J.: The Influence of the Mean Stress on the Propagation of Fatigue Cracks in Aluminum Alloy Sheet. Rep. NLR-TN-M-2111, National Aero- and Astronautical Res. Inst., Amsterdam, Jan. 1963.
3. Forman, R. G.; Kearney, V. E.; and Engle, R. M.: Numerical Analysis of Crack Propagation in Cyclic-Loaded Structures. J. Basic Eng., vol. 89, no. 3, Sept. 1967, pp. 459-464.
4. Hudson, C. M.; and Scardina, J. T.: Effect of Stress Ratio on Fatigue-Crack Growth in 7075-T6 Aluminum-Alloy Sheet. Paper presented at the National Symposium on Fracture Mechanics, Bethlehem, Pa., June 19-21, 1967.
5. Pierce, William S.: Crack Growth in 2014-T6 Aluminum Tensile and Tank Specimens Cyclically Loaded at Cryogenic Temperatures. NASA TN D-4541, 1968.
6. Orange, Thomas W.: Fracture Toughness of Wide 2014-T6 Aluminum Sheet at -320° F. NASA TN D-4017, 1967.
7. Sullivan, Timothy L.; and Orange, Thomas W.: Continuity Gage Measurement of Crack Growth on Flat and Curved Surfaces at Cryogenic Temperatures. NASA TN D-3747, 1966.
8. Paris, Paul C.; and Sih, George C.: Stress Analysis of Cracks. Fracture Toughness Testing and Its Applications. Spec. Tech. Publ. No. 381, ASTM, 1965, pp. 30-83.
9. Isida, Makoto; and Itagaki, Yoshio: Stress Concentration at the Tip of a Central Transverse Crack in a Stiffened Plate Subjected to Tension. Proceedings of the Fourth U. S. National Congress of Applied Mechanics. Vol. 2. ASME, 1962, pp. 955-969.
10. Brown, William F., Jr.; and Srawley, John E.: Plane Strain Crack Toughness Testing of High Strength Metallic Materials. Spec. Tech. Publ. No. 410, ASTM, 1967, p. 77.

TABLE I. - MATERIAL PROPERTIES

(a) U. S. Customary Units

Temperature, °F	0.2 Percent offset yield strength, σ_{ys} , ksi	Ultimate tensile strength, ksi	Elastic modulus, E, ksi	Critical stress intensity, K_c , ksi $\sqrt{\text{in.}}$	Nominal fracture toughness, K_{cn} , ksi $\sqrt{\text{in.}}$	Cyclic critical stress intensity, K_{cc} , ksi $\sqrt{\text{in.}}$
70	65.0	72.3	10.4×10^3	----	----	----
-320	75.2	86.7	11.5	66.2	42.7	69.0

(b) SI Units

Temperature, K	0.2 Percent offset yield strength, σ_{ys} , MN/cm ²	Ultimate tensile strength, MN/cm ²	Elastic modulus, E, gN/m ²	Critical stress intensity, K_c , MN/m ^{3/2}	Nominal fracture toughness, K_{cn} , MN/m ^{3/2}	Cyclic critical stress intensity, K_{cc} , MN/m ^{3/2}
293	44.8	49.9	71.7	----	----	----
77	51.8	59.7	79.3	72.8	46.9	75.8

TABLE II. - CRACK GROWTH DATA FOR 2014-T6 ALUMINUM AT -320° F (77 K)

(a) U. S. Customary Units

Specimen	Crack length 2a, in.	Number of load cycles, N	Crack growth rate, da/dN, in./cycle	Stress intensity factor, K, ksi $\sqrt{\text{in.}}$		Change in stress intensity factor, ΔK	Specimen	Crack length 2a, in.	Number of load cycles, N	Crack growth rate, da/dN, in./cycle	Stress intensity factor, K, ksi $\sqrt{\text{in.}}$		Change in stress intensity factor, ΔK
				Maximum	Minimum						Maximum	Minimum	
				1	0.32 .34 .37 .42 .45 .49 .56 .62 .75 .85						0 800 1600 2400 2800 3200 3600 3800 4000 4016	0.016×10^{-3} .018 .022 .034 .044 .062 .109 .170 1.078 25.0	
2	0.31 .33 .36 .40 .44 .48 .55 .59 .66 .83	0 800 1600 2400 2800 3200 3600 3800 4000 4092	0.012×10^{-3} .015 .021 .036 .050 .064 .102 .121 .261 12.25	37.8×10^3 39.2 40.9 43.4 45.4 47.9 51.6 54.2 58.3 68.1	26.9×10^3 27.8 28.9 30.7 32.1 33.8 36.3 38.0 40.7 46.7	11.0×10^3 11.4 11.9 12.7 13.3 14.1 15.3 16.2 17.6 21.4	6	0.31 .34 .38 .41 .45 .50 .54 .59 .64 .77	0 20 40 60 80 100 110 120 125 130	0.912×10^{-3} .875 .862 .850 .937 1.55 2.31 3.57 6.98 21.00	37.7×10^3 39.9 42.0 44.1 46.0 48.9 50.9 54.2 57.0 64.3	8.4×10^3 8.9 9.4 9.8 10.2 10.8 11.2 11.9 12.4 13.8	29.3×10^3 31.0 32.7 34.3 35.8 38.1 39.7 42.4 44.6 50.6
3	0.32 .34 .38 .40 .43 .46 .50 .57 .73 .84	0 50 100 150 200 250 300 350 400 404	0.260×10^{-3} .285 .290 .285 .290 .350 .530 .910 5.410 20.0	38.3×10^3 39.9 41.8 43.4 45.1 46.7 49.2 53.2 62.2 68.7	17.4×10^3 18.2 19.0 19.7 20.4 21.1 22.2 23.8 27.4 29.8	20.8×10^3 21.8 22.8 23.7 24.7 25.6 27.0 29.3 34.8 38.9	7	0.31 .35 .38 .42 .44 .47 .51 .59 .67 .80	0 10 20 30 35 40 45 50 53 55	1.94×10^{-3} 1.80 1.75 2.02 2.45 3.40 5.20 10.8 20.2 49.5	37.7×10^3 40.1 42.3 44.3 45.6 47.4 49.6 54.1 58.7 66.2	0.0 ↓ ↓ ↓ ↓ ↓ ↓ ↓ ↓ ↓	37.7×10^3 40.1 42.3 44.3 45.6 47.4 49.6 54.1 58.7 66.2
4	0.31 .35 .39 .43 .48 .57 .60 .62 .68 1.00	0 100 200 300 400 500 525 550 575 584	0.100×10^{-3} .102 .100 .105 .155 .290 .375 .575 1.612 18.8	37.7×10^3 40.2 42.7 45.0 48.0 52.9 54.8 55.7 58.8 80.2	17.2×10^3 18.3 19.4 20.4 21.7 23.7 24.5 24.9 26.1 33.4	20.6×10^3 21.9 23.3 24.6 26.3 29.1 30.3 30.8 32.7 46.8	8	0.30 .33 .36 .40 .44 .48 .54 .60 .67 .74	0 10 20 30 40 50 60 65 68 69	1.42×10^{-3} 1.55 1.68 1.80 1.92 2.25 4.40 8.70 18.8 40.0	37.2×10^3 39.2 41.2 43.3 45.4 47.8 51.6 54.9 58.7 62.6	0.0 ↓ ↓ ↓ ↓ ↓ ↓ ↓ ↓ ↓	37.2×10^3 39.2 41.2 43.3 45.4 47.8 51.6 54.9 58.7 62.6

TABLE II. - Continued. CRACK GROWTH DATA FOR 2014-T6 ALUMINUM AT -320° F (77 K)

(a) Continued. U. S. Customary Units

Specimen	Crack length, 2a, in.	Number of load cycles, N	Crack growth rate, da/dN, in./cycle	Stress intensity factor, K, ksi $\sqrt{\text{in.}}$		Change in stress intensity factor, ΔK	Specimen	Crack length, 2a, in.	Number of load cycles, N	Crack growth rate, da/dN, in./cycle	Stress intensity factor, K, ksi $\sqrt{\text{in.}}$		Change in stress intensity factor, ΔK
				Maximum	Minimum						Maximum	Minimum	
				9	0.31 .32 .34 .38 .44 .54 .62 .71 .86 1.05	0 1000 2000 3000 4000 5000 5500 5750 5950 5990					0.006×10^{-3} .008 .012 .022 .039 .070 .117 .246 .767 11.0	30.1×10^3 30.9 31.9 33.5 36.2 40.7 44.4 48.0 54.7 63.6	19.3×10^3 19.8 20.4 21.4 23.1 25.9 28.2 30.3 34.3 39.1
10	0.30 .31 .32 .34 .36 .40 .46 .59 .76 1.08	0 1500 3000 4000 5000 6000 7000 8000 8500 8617	0.001×10^{-3} .003 .006 .008 .014 .025 .044 .093 .359 45.8	29.9×10^3 30.2 30.7 31.5 32.5 34.4 37.4 43.0 50.3 65.1	19.1×10^3 19.3 19.7 20.2 20.8 22.0 23.9 27.3 31.7 39.9	10.8×10^3 10.9 11.1 11.3 11.7 12.4 13.5 15.7 18.6 25.2	14	0.31 .34 .37 .40 .46 .52 .60 .66 .80 1.04	0 100 200 300 400 450 500 525 550 560	0.150×10^{-3} .150 .180 .217 .402 .640 1.01 1.52 4.58 36.0	30.2×10^3 31.6 33.1 34.8 37.5 39.7 43.3 45.9 51.8 63.0	7.0×10^3 7.3 7.7 8.0 8.6 9.1 9.9 10.5 11.7 13.8	23.2×10^3 24.3 25.5 26.7 28.8 30.5 33.4 35.4 40.1 49.2
11	0.31 .34 .37 .40 .42 .46 .52 .65 .76 1.09	0 300 600 800 1000 1200 1400 1600 1700 1748	0.040×10^{-3} .051 .057 .067 .081 .115 .214 .439 .800 33.8	30.4×10^3 31.7 33.3 34.4 35.7 37.4 40.1 45.4 50.2 65.7	14.3×10^3 14.9 15.6 16.2 16.8 17.5 18.8 21.1 23.2 29.2	16.1×10^3 16.8 17.6 18.2 18.9 19.8 21.3 24.2 27.0 36.5	15	0.30 .32 .34 .36 .39 .44 .51 .63 .76 1.05	0 100 200 300 400 500 600 700 750 777	0.075×10^{-3} .085 .095 .137 .187 .287 .430 .805 2.16 18.8	29.9×10^3 30.8 31.7 32.7 34.3 36.4 39.6 44.5 50.3 63.5	6.9×10^3 7.1 7.4 7.6 7.9 8.4 9.1 10.2 11.4 13.9	23.0×10^3 23.7 24.4 25.1 26.3 28.0 30.5 34.3 38.9 49.6
12	0.33 .35 .37 .40 .43 .48 .56 .69 .91 1.13	0 200 400 600 800 1000 1200 1400 1500 1509	0.047×10^{-3} .049 .060 .071 .106 .159 .237 .481 3.62 106	31.1×10^3 32.1 33.1 34.4 36.0 38.4 41.7 47.3 56.7 68.0	14.6×10^3 15.1 15.6 16.2 16.9 18.0 19.5 22.0 25.9 30.0	16.4×10^3 17.0 17.5 18.2 19.1 20.4 22.2 25.3 30.8 37.9	16	0.32 .35 .39 .41 .44 .48 .52 .58 .71 .98	0 40 80 100 120 140 160 180 200 208	0.375×10^{-3} .469 .500 .650 .781 1.02 1.28 1.81 6.19 67.5	30.6×10^3 32.4 34.1 35.0 36.4 38.0 39.9 42.6 48.1 60.0	0.0 ↓ ↓ ↓ ↓ ↓ ↓ ↓ ↓ ↓	30.6×10^3 32.4 34.1 35.0 36.4 38.0 39.9 42.6 48.1 60.0

TABLE II. - Continued. CRACK GROWTH DATA FOR 2014-T6 ALUMINUM AT -320° F (77 K)

(a) Continued. U. S. Customary Units

Specimen	Crack length, 2a, in.	Number of load cycles, N	Crack growth rate, da/dN, in./cycle	Stress intensity factor, K, ksi $\sqrt{\text{in.}}$		Change in stress intensity factor, ΔK	Specimen	Crack length, 2a, in.	Number of load cycles, N	Crack growth rate, da/dN, in./cycle	Stress intensity factor, K, ksi $\sqrt{\text{in.}}$		Change in stress intensity factor, ΔK
				Maximum	Minimum						Maximum	Minimum	
17	0.30	0	0.312×10^{-3}	29.9×10^3	0.0	29.9×10^3	21	0.30	0	0.022×10^{-3}	23.1×10^3	5.5×10^3	17.6×10^3
	.33	40	.350	31.2		31.2		.32	400	.029	23.8	5.7	18.1
	.36	80	.425	32.7		32.7		.34	800	.041	24.7	5.9	18.8
	.40	120	.562	34.4		34.4		.39	1200	.066	26.3	6.3	20.0
	.45	160	.637	36.7		36.7		.46	1600	.112	28.8	6.9	21.9
	.52	200	1.26	39.7		39.7		.51	1800	.167	30.6	7.3	23.3
	.58	220	1.89	42.4		42.4		.60	2000	.258	33.3	7.9	25.4
	.72	240	7.56	48.4		48.4		.78	2200	.806	39.2	9.2	29.9
	.84	245	19.0	53.6		53.6		1.00	2280	2.56	46.3	10.8	35.5
	1.02	248	60.0	62.0		62.0		1.33	2303	35.8	59.0	13.2	45.8
	18	0.30	0	0.003×10^{-3}	23.3×10^3	11.2×10^3		12.1×10^3	22	0.32	0	0.021×10^{-3}	23.7×10^3
.32		1000	.007	23.7	11.4	12.3	.33	400		.028	24.4	5.8	18.6
.33		2000	.012	24.4	11.7	12.6	.37	800		.054	25.6	6.1	19.5
.36		3000	.016	25.5	12.3	13.2	.43	1200		.114	27.8	6.6	21.2
.40		4000	.021	26.7	12.8	13.8	.48	1400		.173	29.8	7.1	22.7
.46		5000	.035	28.7	13.8	14.9	.57	1600		.250	32.5	7.7	24.8
.56		6000	.071	32.0	15.4	16.7	.72	1800		.541	37.2	8.8	28.4
.64		6500	.122	34.9	16.7	18.2	.88	1900		1.225	42.5	10.0	32.5
.84		7000	.287	41.0	19.5	21.5	1.06	1950		3.050	48.5	11.2	37.3
1.37		7313	20.0	60.8	37.6	33.3	1.48	1968		78.0	66.8	14.5	52.4
19		0.31	0	0.004×10^{-3}	23.6×10^3	11.4×10^3	12.2×10^3	23		0.32	0	0.055×10^{-3}	23.7×10^3
	.33	1000	.007	24.2	11.7	12.5	.34		200	.057	24.5		24.5
	.35	2000	.015	24.9	12.0	12.9	.36		400	.075	25.4		25.4
	.39	3000	.020	26.3	12.7	13.6	.40		600	.107	26.8		26.8
	.43	4000	.027	27.9	13.4	14.4	.45		800	.162	28.6		28.6
	.50	5000	.047	30.3	14.6	15.7	.54		1000	.257	31.4		31.4
	.64	6000	.119	34.6	16.6	18.0	.59		1100	.347	33.3		33.3
	.80	6500	.205	39.6	18.9	20.7	.68		1200	.607	35.9		35.9
	1.10	6900	1.12	49.9	23.4	26.5	.99		1300	4.02	45.9		45.9
	1.50	6985	31.4	68.0	30.0	38.0	1.28		1317	41.7	56.7		56.7
	20	0.32	0	0.016×10^{-3}	23.8×10^3	5.7×10^3	18.1×10^3		24	0.32	0	0.035×10^{-3}	23.7×10^3
.34		400	.031	24.4	5.8	18.6	.34	200		.061	24.5		24.5
.38		800	.064	25.9	6.2	19.7	.37	400		.111	25.9		25.9
.44		1200	.102	28.2	6.7	21.4	.43	600		.166	27.8		27.8
.49		1400	.144	29.8	7.1	22.7	.51	800		.271	30.7		30.7
.56		1600	.220	32.2	7.7	24.6	.59	900		.444	33.1		33.1
.70		1800	.495	36.4	8.6	27.8	.72	1000		1.20	37.3		37.3
.83		1900	.931	40.7	9.6	31.2	.92	1050		3.52	43.8		43.8
.96		1950	1.76	44.9	10.5	34.4	1.05	1060		13.1	48.0		48.0
1.37		1986	87.5	60.8	13.5	47.3	1.38	1067		150.0	61.4		61.4

TABLE II. - Continued. CRACK GROWTH DATA FOR 2014-T6 ALUMINUM AT -320° F (77 K)

(a) Continued. U. S. Customary Units

Specimen	Crack length, 2a, in.	Number of load cycles, N	Crack growth rate, da/dN, in./cycle	Stress intensity factor, K, ksi $\sqrt{\text{in.}}$		Change in stress intensity factor, ΔK	Specimen	Crack length, 2a, in.	Number of load cycles, N	Crack growth rate, da/dN, in./cycle	Stress intensity factor, K, ksi $\sqrt{\text{in.}}$		Change in stress intensity factor, ΔK
				Maximum	Minimum						Maximum	Minimum	
25	0.29	0	0.424×10^{-3}	36.5×10^3	3.2×10^3	33.2×10^3	29	0.35	0	1.05×10^{-3}	39.9×10^3	3.5×10^3	36.4×10^3
	.35	28	.763	40.2	3.6	36.6		.40	11	1.70	43.3	3.8	39.4
	.40	52	1.25	43.2	3.8	39.4		.45	23	2.64	46.2	4.1	42.1
	.45	72	2.06	46.1	4.1	42.1		.50	30	4.10	49.0	4.3	44.7
	.50	85	3.38	49.0	4.3	44.7		.55	36	6.37	51.8	4.5	47.3
	.55	89	5.56	51.8	4.5	47.2		.60	40	9.90	54.6	4.8	50.0
	.60	93	9.14	54.6	4.8	49.8		.65	41	15.4	57.4	5.0	52.4
	.65	95	15.0	57.4	5.0	52.4		.70	43	23.9	60.3	5.2	55.1
	.70	96	24.7	60.2	5.2	55.0		.75	43	37.1	63.2	5.4	57.8
	.79	97	60.3	65.5	5.6	60.0		.81	44	62.9	66.8	5.6	61.2
26	0.32	0	0.632×10^{-3}	38.1×10^3	3.4×10^3	34.7×10^3	30	0.38	0	1.55×10^{-3}	42.4×10^3	3.8×10^3	38.6×10^3
	.35	14	.884	40.2	3.6	36.7		.40	1	1.78	43.3	3.8	39.4
	.40	31	1.45	43.3	3.8	39.4		.45	2	2.84	46.2	4.1	42.1
	.45	42	2.37	46.2	4.1	42.1		.50	8	4.53	49.0	4.3	44.7
	.50	53	3.87	49.0	4.3	44.7		.55	13	7.21	51.8	4.5	47.3
	.55	58	6.34	51.8	4.5	47.3		.60	16	11.5	54.6	4.8	49.9
	.60	60	10.4	54.6	4.8	49.9		.65	18	18.3	57.4	5.0	52.4
	.65	62	17.0	57.4	5.0	52.5		.70	19	29.1	60.3	5.2	55.1
	.70	64	27.8	60.3	5.2	55.1		.75	20	46.3	63.2	5.4	57.8
	.73	65	37.3	62.0	5.3	56.7							
27	0.34	0	0.752×10^{-3}	39.6×10^3	3.5×10^3	36.1×10^3	31	0.34	0	1.83×10^{-3}	39.8×10^3	3.5×10^3	36.2×10^3
	.35	3	.838	40.3	3.6	36.7		.35	1	1.96	40.2	3.6	36.7
	.40	17	1.37	43.3	3.8	39.5		.40	6	2.99	43.3	3.8	39.4
	.45	28	2.24	46.2	4.1	42.1		.45	11	4.57	46.2	4.1	42.1
	.50	38	3.67	49.0	4.3	44.7		.50	17	6.99	49.0	4.3	44.7
	.55	44	6.00	51.8	4.5	47.3		.55	21	10.7	51.8	4.5	47.3
	.60	48	9.82	54.6	4.8	49.9		.60	22	16.3	54.6	4.8	49.8
	.65	50	16.1	57.4	5.0	52.5		.65	23	24.9	57.4	5.0	52.4
	.70	51	26.3	60.3	5.2	55.1		.70	24	38.1	60.3	5.2	55.1
	.74	52	38.9	62.6	5.4	57.3		.75	25	58.3	63.2	5.4	57.8
28	0.34	0	0.663×10^{-3}	39.6×10^3	3.5×10^3	36.0×10^3	32	0.33	0	1.31×10^{-3}	39.0×10^3	3.5×10^3	35.5×10^3
	.35	4	.742	40.2	3.6	36.7		.40	9	2.42	43.3	3.8	39.4
	.40	16	1.24	43.2	3.8	39.4		.45	18	3.75	46.2	4.1	42.1
	.45	32	2.08	46.1	4.1	42.1		.50	23	5.81	49.0	4.3	44.7
	.50	42	3.47	49.0	4.3	44.7		.55	28	9.00	51.8	4.5	47.3
	.55	47	5.80	51.8	4.5	47.3		.60	30	14.0	54.6	4.8	49.9
	.60	52	9.69	54.6	4.8	49.8		.65	31	21.6	57.4	5.0	52.4
	.65	54	16.2	57.4	5.0	52.4		.70	32	33.5	60.3	5.2	55.1
	.70	55	27.1	60.2	5.2	55.0		.75	32	52.0	63.2	5.4	57.8
	.74	56	40.9	62.6	5.3	57.2		.76	33	56.7	63.8	5.4	58.3

TABLE II. - Continued. CRACK GROWTH DATA FOR 2014-T6 ALUMINUM AT -320° F (77 K)

(a) Continued. U. S. Customary Units

Specimen	Crack length, 2a, in.	Number of load cycles, N	Crack growth rate, da/dN, in./cycle	Stress intensity factor, K, ksi $\sqrt{\text{in.}}$		Change in stress intensity factor, ΔK	Specimen	Crack length, 2a, in.	Number of load cycles, N	Crack growth rate, da/dN, in./cycle	Stress intensity factor, K, ksi $\sqrt{\text{in.}}$		Change in stress intensity factor, ΔK
				Maximum	Minimum						Maximum	Minimum	
33	0.32	0	1.39×10^{-3}	38.6×10^3	3.4×10^3	35.1×10^3	37	0.30	0	0.135×10^{-3}	29.7×10^3	2.7×10^3	27.0×10^3
	.35	8	1.74	40.2	3.6	36.7		.40	281	.282	34.6	3.2	31.4
	.40	16	2.62	43.3	3.8	39.4		.50	374	.591	39.1	3.6	35.5
	.45	24	3.94	46.2	4.1	42.1		.60	435	1.24	43.3	4.0	39.4
	.50	29	5.92	49.0	4.3	44.7		.70	465	2.59	47.6	4.3	43.3
	.55	32	8.91	51.8	4.5	47.3		.80	478	5.43	51.8	4.7	47.2
	.60	36	13.4	54.6	4.8	49.8		.90	486	11.4	56.3	5.0	51.3
	.65	37	20.2	57.4	5.0	52.4		1.00	488	23.8	61.0	5.4	55.7
	.70	38	30.4	60.3	5.2	55.1		1.10	489	49.9	66.3	5.7	60.6
	.76	39	49.6	63.8	5.4	58.3		1.13	490	62.3	68.0	5.8	62.2
34	0.35	0	1.53×10^{-3}	40.4×10^3	3.6×10^3	36.5×10^3	38	0.31	0	0.116×10^{-3}	30.3×10^3	2.8×10^3	27.5×10^3
	.40	6	2.33	43.3	3.8	39.4		.40	227	.228	34.6	3.2	31.4
	.45	10	3.47	46.2	4.1	42.1		.50	386	.489	39.1	3.6	35.5
	.50	19	5.16	49.0	4.3	44.7		.60	456	1.05	43.4	4.0	39.4
	.55	24	7.68	51.8	4.5	47.3		.70	487	2.25	47.6	4.3	43.3
	.60	26	11.4	54.6	4.8	49.9		.80	503	4.83	51.9	4.7	47.2
	.65	28	17.0	57.4	5.0	52.4		.90	511	10.4	56.3	5.0	51.3
	.70	29	25.3	60.3	5.2	55.1		1.00	514	22.3	61.1	5.4	55.7
	.75	30	37.7	63.2	5.4	57.8		1.10	515	47.8	66.3	5.7	60.6
	.76	31	40.9	63.8	5.4	58.3		1.14	516	64.8	68.6	5.9	62.7
35	0.32	0	0.140×10^{-3}	30.8×10^3	2.8×10^3	28.0×10^3	39	0.30	0	0.116×10^{-3}	29.5×10^3	2.7×10^3	26.7×10^3
	.40	229	.248	34.6	3.2	31.4		.40	326	.268	34.6	3.2	31.4
	.50	375	.515	39.1	3.6	35.5		.50	428	.593	39.1	3.6	35.5
	.60	444	1.07	43.3	4.0	39.4		.60	490	1.31	43.4	4.0	39.4
	.70	478	2.22	47.6	4.3	43.2		.70	518	2.90	47.6	4.3	43.3
	.80	496	4.61	51.8	4.7	47.2		.80	529	6.42	51.9	4.7	47.2
	.90	504	9.56	56.3	5.0	51.3		.90	534	14.2	56.3	5.0	51.3
	1.00	508	19.9	61.0	5.4	55.7		1.00	536	31.4	61.1	5.4	55.7
	1.10	509	41.2	66.3	5.7	60.6		1.05	537	46.8	63.6	5.5	58.1
	1.18	510	74.0	71.0	6.0	65.0		1.08	537	59.4	65.2	5.6	59.6
36	0.34	0	0.161×10^{-3}	31.8×10^3	2.9×10^3	28.8×10^3	40	0.34	0	0.179×10^{-3}	31.6×10^3	2.9×10^3	28.7×10^3
	.40	104	.251	34.6	3.2	31.4		.40	86	.301	34.6	3.2	31.4
	.50	210	.531	39.1	3.6	35.5		.50	199	.693	39.1	3.6	35.5
	.60	277	1.12	43.4	4.0	39.4		.60	255	1.60	43.3	4.0	39.4
	.70	312	2.38	47.6	4.3	43.3		.70	277	3.68	47.6	4.3	43.2
	.80	329	5.04	51.9	4.7	47.2		.80	284	8.46	51.8	4.7	47.2
	.90	337	10.7	56.3	5.0	51.3		.85	287	12.8	54.0	4.8	49.2
	1.00	340	22.6	61.1	5.4	55.7		.90	289	19.5	56.3	5.0	51.3
	1.05	341	32.8	63.6	5.5	58.7		.95	290	29.6	58.6	5.2	53.4
	1.10	342	47.7	66.3	5.7	60.6		1.04	291	62.7	63.0	5.5	57.5

TABLE II. - Continued. CRACK GROWTH DATA FOR 2014-T6 ALUMINUM AT -320° F (77 K)

(a) Continued. U. S. Customary Units

Specimen	Crack length, 2a, in.	Number of load cycles, N	Crack growth rate, da/dN, in./cycle	Stress intensity factor, K, ksi√in.		Change in stress intensity factor, ΔK	Specimen	Crack length, 2a, in.	Number of load cycles, N	Crack growth rate, da/dN, in./cycle	Stress intensity factor, K, ksi√in.		Change in stress intensity factor, ΔK
				Maximum	Minimum						Maximum	Minimum	
41	0.35	0	0.266×10 ⁻³	32.3×10 ³	3.0×10 ³	29.3×10 ³	45	0.34	0	0.051×10 ⁻³	24.5×10 ³	2.3×10 ³	22.2×10 ³
	.40	49	.391	34.6	3.2	31.4		.45	830	.105	28.6	2.7	25.8
	.50	147	.843	39.1	3.6	35.5		.60	1207	.276	33.5	3.2	30.3
	.60	192	1.82	43.4	4.0	39.5		.75	1367	.727	38.2	3.6	34.6
	.70	209	3.92	47.7	4.3	43.3		.90	1437	1.91	42.9	4.0	38.9
	.80	217	8.47	51.9	4.7	47.3		1.00	1455	3.65	46.2	4.3	42.0
	.90	220	18.3	56.4	5.0	51.4		1.10	1467	6.95	49.7	4.6	45.1
	.95	221	26.8	58.7	5.2	53.5		1.20	1474	13.3	53.5	4.9	48.6
	1.00	222	39.4	61.2	5.4	55.8		1.30	1477	25.3	57.6	5.2	52.4
	1.11	223	91.9	67.0	5.8	61.2		1.39	1478	45.1	61.8	5.4	56.4
	42	0.36	0	0.146×10 ⁻³	32.7×10 ³	3.0×10 ³		29.7×10 ³	46	0.37	0	0.086×10 ⁻³	25.8×10 ³
.40		39	.203	34.6	3.2	31.4	.40	233		.104	26.8	2.6	24.3
.50		161	.464	39.1	3.6	35.5	.60	726		.377	33.5	3.2	30.3
.60		232	1.06	43.3	4.0	39.4	.80	884		1.37	39.8	3.7	36.1
.70		260	2.42	47.6	4.3	43.2	.90	913		2.60	43.0	4.0	39.0
.80		280	5.54	51.8	4.7	47.2	1.00	930		4.95	46.3	4.3	42.0
.85		284	8.37	54.0	4.8	49.2	1.10	938		9.43	49.7	4.6	45.2
.90		288	12.6	56.3	5.0	51.3	1.20	942		18.0	53.5	4.9	48.6
.95		290	19.1	58.6	5.2	53.4	1.35	944		47.2	59.9	5.3	54.6
1.03		291	37.0	62.5	5.5	57.1	1.44	945		84.2	64.5	5.6	58.9
43		0.32	0	0.357×10 ⁻³	30.9×10 ³	2.9×10 ³	28.0×10 ³	47		0.34	0	0.058×10 ⁻³	24.6×10 ³
	.35	41	.455	32.2	3.0	29.2	.45		737	.116	28.5	2.7	25.8
	.40	92	.710	34.6	3.2	31.4	.60		1131	.301	33.4	3.2	30.3
	.45	131	1.11	36.8	3.4	33.4	.75		1279	.777	38.2	3.6	34.6
	.50	145	1.74	39.0	3.6	35.5	.90		1337	2.01	42.9	4.0	38.9
	.60	162	4.24	43.3	4.0	39.4	1.05		1363	5.19	47.9	4.4	43.5
	.70	171	10.3	47.5	4.3	43.2	1.15		1375	9.76	51.5	4.7	46.8
	.75	173	16.2	49.7	4.5	45.2	1.25		1379	18.4	55.4	5.0	50.4
	.85	174	39.5	54.0	4.8	49.2	1.35		1380	34.6	59.8	5.3	54.5
	.94	175	88.2	58.1	5.1	53.0	1.43		1381	57.4	63.8	5.6	58.3
	44	0.34	0	0.216×10 ⁻³	31.8×10 ³	2.9×10 ³	28.8×10 ³		48	0.36	0	0.059×10 ⁻³	25.4×10 ³
.40		86	.348	34.6	3.2	31.4	.40	277		.076	26.8	2.5	24.2
.50		184	.779	39.0	3.6	35.5	.50	716		.145	30.2	2.9	27.3
.60		229	1.74	43.3	4.0	39.4	.60	880		.279	33.4	3.2	30.3
.70		247	3.91	47.5	4.3	43.2	.80	1101		1.02	39.7	3.7	36.0
.80		255	8.74	51.8	4.7	47.2	1.00	1155		3.76	46.2	4.3	41.9
.85		258	13.1	54.0	4.8	49.2	1.10	1167		7.20	49.7	4.6	45.1
.90		259	19.6	56.3	5.0	51.2	1.20	1174		13.8	53.4	4.9	48.6
.95		261	29.3	58.6	5.2	53.4	1.30	1177		26.5	57.5	5.2	52.4
1.02		262	51.5	62.0	5.4	56.6	1.36	1178		39.1	60.3	5.3	55.0

TABLE II. - Continued. CRACK GROWTH DATA FOR 2014-T6 ALUMINUM AT -320° F (77 K)

(a) Concluded. U. S. Customary Units

Specimen	Crack length, 2a, in.	Number of load cycles, N	Crack growth rate, da/dN, in./cycle	Stress intensity factor, K, ksi $\sqrt{\text{in.}}$		Change in stress intensity factor, ΔK	Specimen	Crack length, 2a, in.	Number of load cycles, N	Crack growth rate, da/dN, in./cycle	Stress intensity factor, K, ksi $\sqrt{\text{in.}}$		Change in stress intensity factor, ΔK
				Maximum	Minimum						Maximum	Minimum	
				49	0.35						0	0.049×10^{-3}	
	.50	966	.123	30.2	2.9	27.4		.45	688	.100	28.6	2.7	25.8
	.70	1340	.399	36.6	3.5	33.2		.60	1049	.255	33.5	3.2	30.3
	.90	1476	1.30	42.9	4.0	38.9		.70	1169	.475	36.6	3.6	33.2
	1.00	1519	2.34	46.2	4.3	41.9		.80	1244	.885	39.8	3.7	36.0
	1.10	1539	4.23	49.7	4.6	45.1		.90	1291	1.65	42.9	4.0	38.9
	1.20	1550	7.64	53.4	4.9	48.6		1.00	1319	3.08	46.2	4.3	41.9
	1.30	1555	13.8	57.6	5.2	52.4		1.15	1336	7.84	51.5	4.7	46.8
	1.40	1558	24.9	62.3	5.5	56.8		1.25	1342	14.6	55.5	5.0	50.4
	1.48	1559	39.9	66.8	5.7	61.0		1.35	1346	27.2	59.9	5.3	54.6
50	0.34	0	0.047×10^{-3}	24.8×10^3	2.4×10^3	22.4×10^3	53	0.36	0	0.090×10^{-3}	25.2×10^3	2.4×10^3	22.8×10^3
	.40	525	.069	26.8	2.5	24.3		.50	662	.230	30.2	2.9	27.4
	.50	870	.137	30.2	2.9	27.4		.65	840	.618	35.0	3.3	31.7
	.60	1033	.273	33.5	3.2	30.3		.75	899	1.19	38.2	3.5	34.6
	.70	1156	.542	36.6	3.6	33.2		.85	931	2.31	41.3	3.9	37.5
	.80	1231	1.08	39.8	3.7	36.0		.95	948	4.46	44.6	4.1	40.4
	.90	1275	2.14	42.9	4.0	38.9		1.05	956	8.61	47.9	4.4	43.5
	1.05	1303	5.98	47.9	4.4	43.5		1.15	962	16.6	51.5	4.7	46.8
	1.20	1312	16.7	53.5	4.9	48.6		1.25	964	32.1	55.5	5.0	50.4
	1.34	1314	43.7	59.4	5.3	54.1		1.35	965	62.0	59.9	5.3	54.6
51	0.38	0	0.050×10^{-3}	26.1×10^3	2.5×10^3	23.6×10^3	54	0.36	0	0.047×10^{-3}	25.4×10^3	2.4×10^3	23.0×10^3
	.45	441	.080	28.6	2.7	25.8		.50	726	.118	30.2	2.9	27.4
	.60	971	.214	33.5	3.2	30.3		.65	1031	.323	35.0	3.3	31.7
	.75	1148	.571	38.2	3.5	34.6		.80	1174	.880	39.7	3.7	36.0
	.90	1235	1.53	42.9	4.0	38.9		.90	1223	1.72	42.9	4.0	38.9
	1.00	1261	2.94	46.2	4.3	41.9		1.00	1248	3.35	46.2	4.3	41.9
	1.10	1283	5.67	49.7	4.6	45.1		1.10	1269	6.54	49.7	4.6	45.1
	1.20	1290	10.9	53.4	4.9	48.6		1.20	1273	12.8	53.4	4.9	48.6
	1.30	1294	21.0	57.6	5.2	52.4		1.30	1275	24.9	57.6	5.2	52.4
	1.37	1295	33.3	60.8	5.4	55.4		1.40	1276	48.7	62.3	5.5	56.8

TABLE II. - Continued. CRACK GROWTH DATA FOR 2014-T6 ALUMINUM AT -320° F (77 K)

(b) SI Units

Specimen	Crack length, 2a, cm	Number of load cycles, N	Crack growth rate, da/dN, cm/cycle	Stress intensity factor, K, MN/m ^{3/2}		Change in stress intensity factor, ΔK	Specimen	Crack length, 2a, cm	Number of load cycles, N	Crack growth rate, da/dN, cm/cycle	Stress intensity factor, K, MN/m ^{3/2}		Change in stress intensity factor, ΔK
				Maximum	Minimum						Maximum	Minimum	
1	0.81	0	0.040×10 ⁻³	42.0×10 ³	29.8×10 ³	12.2×10 ³	5	0.86	0	0.810×10 ⁻³	43.5×10 ³	9.7×10 ³	33.8×10 ³
	.87	800	.046	43.8	31.0	12.7		.93	20	.873	45.2	10.1	35.1
	.95	1600	.057	45.9	32.5	13.4		.99	40	.857	46.9	10.4	36.4
	1.07	2400	.087	48.9	34.6	14.3		1.07	60	.952	48.8	10.8	38.0
	1.15	2800	.113	50.9	35.9	14.9		1.14	80	1.10	50.7	11.2	39.5
	1.25	3200	.159	53.5	37.7	15.8		1.25	100	1.59	53.4	11.8	41.6
	1.42	3600	.276	57.5	40.4	17.1		1.40	120	2.22	57.0	12.5	44.5
	1.56	3800	.433	61.0	42.7	18.3		1.50	130	2.84	59.5	13.0	46.4
	1.90	4000	2.74	69.4	48.1	21.3		1.69	140	7.94	64.1	13.9	50.2
	2.16	4016	63.5	76.2	52.1	24.1		2.16	146	52.4	76.2	16.1	60.1
	2	0.80	0	0.030×10 ⁻³	41.7×10 ³	29.6×10 ³		12.1×10 ³	6	0.79	0	2.32×10 ⁻³	41.4×10 ³
.85		800	.037	43.1	30.5	12.5	.88	20		2.22	43.9	9.8	34.1
.91		1600	.052	44.9	31.8	13.1	.97	40		2.19	46.2	10.3	35.9
1.02		2400	.090	47.7	33.7	13.9	1.05	60		2.16	48.4	10.8	37.6
1.11		2800	.128	49.9	35.3	14.6	1.14	80		2.38	50.6	11.2	39.4
1.22		3200	.162	52.7	37.1	15.5	1.27	100		3.94	53.8	11.9	41.9
1.39		3600	.259	56.7	39.9	16.8	1.36	110		5.87	56.0	12.3	43.6
1.51		3800	.307	59.6	41.8	17.8	1.51	120		9.06	59.6	13.1	46.5
1.69		4000	.662	64.0	44.7	19.4	1.63	125		17.7	62.6	13.7	49.0
2.11		4092	31.1	74.8	51.3	23.5	1.96	130		53.3	70.7	15.1	55.6
3		0.81	0	0.660×10 ⁻³	42.0×10 ³	19.1×10 ³	22.9×10 ³	7		0.78	0	4.92×10 ⁻³	41.4×10 ³
	.88	50	.724	43.9	20.0	23.9	.88		10	4.57	44.1		44.1
	.95	100	.737	45.9	20.9	25.0	.98		20	4.44	46.5		46.5
	1.02	150	.724	47.7	21.7	26.1	1.06		30	5.14	48.7		48.7
	1.10	200	.737	49.6	22.5	27.1	1.12		35	6.22	50.1		50.1
	1.17	250	.889	51.4	23.2	28.1	1.20		40	8.64	52.1		52.1
	1.28	300	1.35	54.1	24.4	29.7	1.30		45	13.2	54.5		54.5
	1.46	350	2.31	58.4	26.2	32.2	1.50		50	27.3	59.4		59.4
	1.86	400	13.7	68.3	30.1	38.2	1.71		53	51.4	64.5		64.5
	2.13	404	50.8	75.5	32.7	42.8	2.03		55	126	72.8		72.8
	4	0.79	0	0.254×10 ⁻³	41.5×10 ³	18.9×10 ³	22.6×10 ³		8	0.77	0	3.62×10 ⁻³	40.9×10 ³
.89		100	.260	44.2	20.1	24.1	.85	10		3.94	43.1		43.1
.99		200	.254	46.9	21.3	25.6	.93	20		4.25	45.2		45.2
1.09		300	.267	49.5	22.4	27.1	1.02	30		4.57	47.5		47.5
1.22		400	.394	52.7	23.8	28.9	1.11	40		4.89	49.9		49.9
1.45		500	.737	58.1	26.1	32.0	1.21	50		5.72	52.5		52.5
1.53		525	.952	60.2	26.9	33.3	1.38	60		11.2	56.6		56.6
1.57		550	1.46	61.2	27.4	33.9	1.54	65		22.1	60.3		60.3
1.71		575	4.10	64.7	28.7	35.9	1.71	68		47.6	64.5		64.5
2.54		584	47.6	88.2	36.7	51.5	1.88	69		60.8	68.8		68.8

TABLE II. - Continued. CRACK GROWTH DATA FOR 2014-T6 ALUMINUM AT -320° F (77 K)

(b) Continued. SI Units

Specimen	Crack length, 2a, cm	Number of load cycles, N	Crack growth rate, da/dN, cm/cycle	Stress intensity factor, K, MN/m ^{3/2}		Change in stress intensity factor, ΔK	Specimen	Crack length, 2a, cm	Number of load cycles, N	Crack growth rate, da/dN, cm/cycle	Stress intensity factor, K, MN/m ^{3/2}		Change in stress intensity factor, ΔK
				Maximum	Minimum						Maximum	Minimum	
9	0.78	0	0.016×10 ⁻³	33.1×10 ³	21.2×10 ³	11.9×10 ³	13	0.77	0	0.063×10 ⁻³	32.9×10 ³	15.5×10 ³	17.4×10 ³
	.82	1000	.021	34.0	21.7	12.3		.83	400	.079	34.2	16.1	18.1
	.87	2000	.030	35.0	22.4	12.6		.90	800	.124	35.7	16.8	18.9
	.96	3000	.057	36.8	23.5	13.3		1.03	1200	.203	38.2	17.9	20.3
	1.10	4000	.098	39.8	25.4	14.4		1.25	1600	.361	42.6	19.9	22.6
	1.36	5000	.178	44.7	28.4	16.3		1.43	1800	.537	45.9	21.4	24.5
	1.59	5500	.297	48.8	31.0	17.9		1.71	2000	.972	51.0	23.7	27.3
	1.80	5750	.625	52.8	33.3	19.4		2.00	2100	2.39	56.4	26.0	30.4
	2.20	5950	1.95	60.1	37.6	22.5		2.36	2150	6.22	63.4	28.8	34.6
	2.67	5990	27.8	69.9	42.9	27.0		2.82	2169	54.6	73.5	32.5	41.0
10	0.77	0	0.004×10 ⁻³	32.9×10 ³	21.0×10 ³	11.8×10 ³	14	0.79	0	0.381×10 ⁻³	33.2×10 ³	7.7×10 ³	25.5×10 ³
	.79	1500	.007	33.2	21.2	11.9		.86	100	.381	34.8	8.1	26.7
	.81	3000	.015	33.7	21.6	12.1		.94	200	.457	36.4	8.4	28.0
	.85	4000	.020	34.6	22.2	12.5		1.03	300	.552	38.2	8.8	29.4
	.91	5000	.035	35.7	22.9	12.9		1.18	400	1.02	41.2	9.5	31.7
	1.01	6000	.064	37.8	24.2	13.6		1.31	450	1.63	43.6	10.0	33.6
	1.18	7000	.112	41.1	26.2	14.9		1.52	500	2.57	47.6	10.9	36.7
	1.50	8000	.236	47.2	30.0	17.2		1.68	525	3.86	50.5	11.5	38.9
	1.94	8500	.912	55.3	34.8	20.4		2.03	550	11.6	56.9	12.9	44.1
	2.74	8617	116	71.6	43.8	27.7		2.64	560	91.4	69.2	15.2	54.1
11	0.80	0	0.102×10 ⁻³	33.4×10 ³	15.7×10 ³	17.6×10 ³	15	0.77	0	0.190×10 ⁻³	32.9×10 ³	7.6×10 ³	25.2×10 ³
	.86	300	.130	34.8	16.4	18.4		.82	100	.216	33.9	7.9	26.0
	.94	600	.146	36.5	17.2	19.3		.86	200	.241	34.8	8.1	26.8
	1.01	800	.171	37.8	17.8	20.0		.91	300	.349	35.9	8.3	27.6
	1.08	1000	.206	39.2	18.4	20.8		1.00	400	.476	37.7	8.7	28.9
	1.17	1200	.292	41.1	19.3	21.8		1.12	500	.730	40.0	9.2	30.7
	1.33	1400	.543	44.1	20.7	23.4		1.31	600	1.09	43.6	10.0	33.5
	1.65	1600	1.11	49.8	23.2	26.6		1.60	700	2.04	48.9	11.2	37.7
	1.94	1700	2.03	55.2	25.5	29.7		1.94	750	5.50	55.3	12.5	42.7
	2.77	1748	85.7	72.2	32.1	40.1		2.67	777	47.6	69.8	15.3	54.5
12	0.83	0	0.121×10 ⁻³	34.1×10 ³	16.1×10 ³	18.1×10 ³	16	0.81	0	0.952×10 ⁻³	33.6×10 ³	0.0	33.6×10 ³
	.88	200	.124	35.3	16.6	18.7		.90	40	1.19	35.5		35.5
	.94	400	.152	36.4	17.1	19.3		.99	80	1.27	37.5		37.5
	1.01	600	.181	37.8	17.8	20.0		1.04	100	1.65	38.5		38.5
	1.10	800	.270	39.6	18.6	21.0		1.12	120	1.98	40.0		40.0
	1.23	1000	.403	42.1	19.8	22.4		1.21	140	2.59	41.7		41.7
	1.43	1200	.603	45.8	21.4	24.4		1.32	160	3.25	43.8		43.8
	1.76	1400	1.22	51.9	24.1	27.8		1.48	180	4.59	46.8		46.8
	2.31	1500	9.21	62.3	28.5	33.9		1.81	200	15.7	52.8		52.8
	2.87	1509	270	74.7	33.0	41.7		2.49	208	171	66.0		66.0

TABLE II. - Continued. CRACK GROWTH DATA FOR 2014-T6 ALUMINUM AT -320° F (77 K)

(b) Continued. SI Units

Specimen	Crack length, 2a, cm	Number of load cycles, N	Crack growth rate, da/dN, cm/cycle	Stress intensity factor, K, MN/m ^{3/2}		Change in stress intensity factor, ΔK	Specimen	Crack length, 2a, cm	Number of load cycles, N	Crack growth rate, da/dN, cm/cycle	Stress intensity factor, K, MN/m ^{3/2}		Change in stress intensity factor, ΔK		
				Maximum	Minimum						Maximum	Minimum			
17	0.77	0	0.794×10 ⁻³	32.8×10 ³	0.0	32.8×10 ³	21	0.76	0	0.056×10 ⁻³	25.4×10 ³	6.1×10 ³	19.3×10 ³		
	.84	40	.889	34.3		34.3		.81	400	.075	26.1	6.2	19.9		
	.91	80	1.08	35.9		35.9		.87	800	.105	27.2	6.5	20.7		
	1.00	120	1.43	37.7		37.7		.98	1200	.168	28.9	6.9	22.0		
	1.14	160	1.62	40.4		40.4		1.16	1600	.284	31.6	7.5	24.1		
	1.31	200	3.21	43.6		43.6		1.30	1800	.425	33.6	8.0	25.6		
	1.47	220	4.79	46.6		46.6		1.51	2000	.656	36.6	8.7	27.9		
	1.83	240	19.2	53.2		53.2		1.98	2200	2.05	43.0	10.2	32.9		
	2.13	245	48.3	58.9		58.9		2.54	2280	6.51	50.8	11.8	39.0		
	2.59	248	113	68.2		68.2		3.38	2303	90.8	64.8	14.5	50.3		
18	0.77	0	0.008×10 ⁻³	25.6×10 ³	12.3×10 ³	13.2×10 ³	22	0.80	0	0.052×10 ⁻³	26.1×10 ³	6.2×10 ³	19.8×10 ³		
	.81	1000	.019	26.1	12.6	13.5		.85	400	.071	26.8	6.4	20.4		
	.85	2000	.032	26.8	12.9	13.9		.93	800	.138	28.1	6.7	21.4		
	.92	3000	.040	28.0	13.5	14.5		1.08	1200	.289	30.5	7.3	23.2		
	1.01	4000	.053	29.3	14.1	15.2		1.23	1400	.440	32.7	7.8	24.9		
	1.16	5000	.090	31.6	15.2	16.4		1.45	1600	.635	35.8	8.5	27.2		
	1.41	6000	.180	35.2	16.9	18.3		1.82	1800	1.37	40.9	9.7	31.2		
	1.64	6500	.311	38.3	18.3	20.0		2.25	1900	3.11	46.7	11.0	35.7		
	2.13	7000	.730	45.1	21.4	23.6		2.71	1950	7.75	53.3	12.4	40.9		
	3.48	7313	50.8	66.8	30.3	36.5		3.76	1968	198	73.5	15.9	57.5		
	19	0.80	0	0.011×10 ⁻³	25.9×10 ³	12.5×10 ³		13.4×10 ³	23	0.80	0	0.140×10 ⁻³	26.0×10 ³	0.0	26.0×10 ³
		.83	1000	.018	26.5	12.8		13.7		.86	200	.146	26.9		26.9
		.89	2000	.038	27.4	13.2		14.2		.91	400	.190	27.9		27.9
.98		3000	.051	28.9	13.9	15.0	1.02	600		.273	29.5		29.5		
1.09		4000	.070	30.6	14.7	15.9	1.15	800		.413	31.4		31.4		
1.27		5000	.121	33.2	16.0	17.2	1.36	1000		.654	34.5		34.5		
1.62		6000	.302	38.0	18.2	19.8	1.51	1100		.883	36.6		36.6		
2.02		6500	.521	43.6	20.8	22.8	1.72	1200		1.54	39.4		39.4		
2.81		6900	2.86	54.8	25.7	29.1	2.51	1300		10.2	50.4		50.4		
3.81		6985	79.8	74.7	32.9	41.8	3.25	1317		106	62.3		62.3		
20	0.81	0	0.040×10 ⁻³	26.1×10 ³	6.2×10 ³	19.9×10 ³	24	0.81	0	0.089×10 ⁻³	26.1×10 ³	0.0	26.1×10 ³		
	.85	400	.079	26.9	6.4	20.4		.86	200	.156	26.9		26.9		
	.95	800	.162	28.4	6.8	21.7		.95	400	.283	28.4		28.4		
	1.12	1200	.260	30.9	7.4	23.6		1.09	600	.422	30.6		30.6		
	1.24	1400	.367	32.8	7.8	25.0		1.30	800	.689	33.7		33.7		
	1.43	1600	.560	35.4	8.4	27.0		1.49	900	1.13	36.3		36.3		
	1.77	1800	1.26	40.0	9.5	30.6		1.83	1000	3.04	41.0		41.0		
	2.11	1900	2.36	44.8	10.5	34.2		2.35	1050	8.95	48.1		48.1		
	2.44	1950	4.48	49.3	11.5	37.8		2.67	1060	33.3	52.7		52.7		
	3.48	1986	222	66.8	14.8	51.9		3.51	1067	63.5	67.4		67.4		

TABLE II. - Continued. CRACK GROWTH DATA FOR 2014-T6 ALUMINUM AT -320° F (77 K)

(b) Continued. SI Units

Specimen	Crack length, 2a, cm	Number of load cycles, N	Crack growth rate, da/dN, cm/cycle	Stress intensity factor, K, MN/m ^{3/2}		Change in stress intensity factor, ΔK	Specimen	Crack length, 2a, cm	Number of load cycles, N	Crack growth rate, da/dN, cm/cycle	Stress intensity factor, K, MN/m ^{3/2}		Change in stress intensity factor, ΔK
				Maximum	Minimum						Maximum	Minimum	
25	0.74	0	1.08×10 ⁻³	40.1×10 ³	3.6×10 ³	36.5×10 ³	29	0.88	0	2.66×10 ⁻³	43.9×10 ³	3.9×10 ³	40.0×10 ³
	.89	28	1.94	44.2	3.9	40.3		1.02	11	4.32	47.5	4.2	43.3
	1.02	52	3.18	47.5	4.2	43.3		1.14	23	6.71	50.7	4.5	46.3
	1.14	72	5.23	50.7	4.5	46.2		1.27	30	10.4	53.8	4.7	49.1
	1.27	85	8.60	53.8	4.7	49.1		1.40	36	16.2	56.9	5.0	52.0
	1.40	89	14.1	56.9	5.0	51.9		1.52	40	25.1	60.0	5.2	54.8
	1.52	93	23.2	60.0	5.2	54.7		1.65	41	39.0	63.1	5.5	57.6
	1.65	95	38.1	63.0	5.5	57.6		1.78	43	60.6	66.2	5.7	60.5
	1.78	96	62.7	66.2	5.7	60.5		1.91	43	94.2	69.4	5.9	63.5
	2.01	97	153	72.0	6.1	65.9		2.00	44	160	73.4	6.2	67.2
26	0.80	0	1.61×10 ⁻³	41.9×10 ³	3.7×10 ³	38.2×10 ³	30	0.98	0	3.94×10 ⁻³	46.5×10 ³	4.1×10 ³	42.4×10 ³
	.89	14	2.24	44.2	3.9	40.3		1.02	1	4.53	47.5	4.2	43.3
	1.02	31	3.67	47.5	4.2	43.3		1.14	2	7.22	50.7	4.5	46.3
	1.14	42	6.01	50.7	4.5	46.3		1.27	8	11.5	53.8	4.7	49.1
	1.27	53	9.84	53.9	4.7	49.1		1.40	13	18.3	56.9	5.0	52.0
	1.40	58	16.1	56.9	5.0	52.0		1.52	16	29.2	60.0	5.2	54.8
	1.52	60	26.3	60.0	5.2	54.8		1.65	18	46.4	63.1	5.5	57.6
	1.65	62	43.1	63.1	5.5	57.6		1.78	19	73.9	66.2	5.7	60.5
	1.78	64	70.5	66.2	5.7	60.5		1.90	20	118	69.4	5.9	63.5
	1.85	65	94.7	68.1	5.8	62.3							
27	0.86	0	1.91×10 ⁻³	43.5×10 ³	3.86×10 ³	39.6×10 ³	31	0.87	0	4.64×10 ⁻³	43.7×10 ³	3.9×10 ³	39.8×10 ³
	.89	3	2.13	44.2	3.92	40.3		.89	1	4.97	44.2	3.9	40.3
	1.02	17	3.48	47.6	4.21	43.3		1.02	6	7.60	47.5	4.2	43.3
	1.14	28	5.70	50.8	4.48	46.3		1.14	11	11.6	50.7	4.5	46.2
	1.27	38	9.32	53.9	4.73	49.1		1.27	17	17.7	53.8	4.7	49.1
	1.40	44	15.2	57.0	4.98	52.0		1.40	21	27.1	56.9	5.0	51.9
	1.52	48	24.9	60.0	5.23	54.8		1.52	22	41.4	60.0	5.2	54.8
	1.65	50	40.8	63.1	5.46	57.7		1.65	23	63.4	63.1	5.5	57.6
	1.78	51	66.7	66.3	5.70	60.6		1.78	24	96.8	66.2	5.7	60.5
	1.88	52	98.9	68.8	5.88	62.9		1.90	25	148	69.4	5.9	63.5
28	0.86	0	1.68×10 ⁻³	43.5×10 ³	3.9×10 ³	39.6×10 ³	32	0.84	0	3.32×10 ⁻³	42.9×10 ³	3.8×10 ³	39.1×10 ³
	.89	4	1.89	44.2	3.9	40.3		1.02	9	6.14	47.5	4.2	43.3
	1.02	16	3.15	47.5	4.2	43.3		1.14	18	9.52	50.7	4.5	46.3
	1.14	32	5.27	50.7	4.5	46.2		1.27	23	14.8	53.8	4.7	49.1
	1.27	42	8.81	53.8	4.7	49.1		1.40	28	22.9	56.9	5.0	52.0
	1.40	47	14.7	56.9	5.0	51.9		1.52	30	35.4	60.0	5.2	54.8
	1.52	52	24.6	60.0	5.2	54.7		1.65	31	54.9	63.1	5.5	57.6
	1.65	54	41.2	63.1	5.5	57.6		1.78	32	85.1	66.2	5.7	60.5
	1.78	55	68.8	66.2	5.7	60.5		1.90	32	132	69.4	5.9	63.5
	1.88	56	104	68.7	5.9	62.9		1.93	33	144	70.1	6.0	64.1

TABLE II. - Continued. CRACK GROWTH DATA FOR 2014-T6 ALUMINUM AT -320° F (77 K)

(b) Continued. SI Units

Specimen	Crack length, 2a, cm	Number of load cycles, N	Crack growth rate, da/dN, cm/cycle	Stress intensity factor, K, MN/m ^{3/2}		Change in stress intensity factor, ΔK	Specimen	Crack length, 2a, cm	Number of load cycles, N	Crack growth rate, da/dN, cm/cycle	Stress intensity factor, K, MN/m ^{3/2}		Change in stress intensity factor, ΔK
				Maximum	Minimum						Maximum	Minimum	
33	0.82	0	3.54×10 ⁻³	42.4×10 ³	3.8×10 ³	38.6×10 ³	37	0.76	0	0.342×10 ⁻³	32.7×10 ³	3.0×10 ³	29.6×10 ³
	.89	8	4.41	44.2	3.9	40.3		1.02	281	.717	38.0	3.5	34.5
	1.02	16	6.64	47.5	4.2	43.3		1.27	374	1.50	42.9	3.9	39.0
	1.14	24	10.0	50.7	4.5	46.2		1.52	435	3.15	47.6	4.4	43.3
	1.27	29	15.0	53.8	4.7	49.1		1.78	465	6.59	52.3	4.7	47.5
	1.40	32	22.6	56.9	5.0	51.9		2.03	478	13.8	57.0	5.1	51.8
	1.52	36	34.1	60.0	5.2	54.8		2.29	486	28.9	61.9	5.5	56.3
	1.65	37	51.3	63.1	5.5	57.6		2.54	488	60.6	67.1	5.9	61.2
	1.78	38	77.2	66.2	5.7	60.5		2.79	489	127	72.8	6.3	66.5
	1.93	39	126	70.7	6.0	64.1		2.87	490	158	74.7	6.4	68.3
34	0.88	0	3.88×10 ⁻³	44.0×10 ³	3.9×10 ³	40.1×10 ³	38	0.79	0	0.296×10 ⁻³	33.3×10 ³	3.1×10 ³	30.3×10 ³
	1.02	6	5.92	47.5	4.2	43.3		1.02	227	.579	38.0	3.5	34.5
	1.14	10	8.81	50.7	4.5	46.3		1.27	386	1.24	42.9	3.9	39.0
	1.27	19	13.1	53.8	4.7	49.1		1.52	456	2.67	47.6	4.4	43.3
	1.40	24	19.5	56.9	5.0	52.0		1.78	487	5.72	52.3	4.7	47.5
	1.52	26	29.1	60.0	5.2	54.8		2.03	503	12.3	57.0	5.1	51.9
	1.65	28	43.3	63.1	5.5	57.6		2.29	511	26.3	61.9	5.5	56.4
	1.78	29	64.4	66.2	5.7	60.5		2.54	514	56.5	67.1	5.9	61.2
	1.90	30	95.8	69.4	5.9	63.5		2.79	515	121	72.8	6.3	66.6
	1.93	31	104	70.1	6.0	64.1		2.90	516	165	75.4	6.4	68.9
35	0.82	0	0.356×10 ⁻³	33.9×10 ³	3.1×10 ³	30.7×10 ³	39	0.75	0	0.296×10 ⁻³	32.4×10 ³	3.0×10 ³	29.4×10 ³
	1.02	229	.629	38.0	3.5	34.5		1.02	326	.681	38.0	3.5	34.5
	1.27	375	1.31	42.9	3.9	39.0		1.27	428	1.51	42.9	3.9	39.0
	1.52	444	2.71	47.6	4.4	43.3		1.52	490	3.33	47.6	4.4	43.3
	1.78	478	5.64	52.3	4.7	47.5		1.78	518	7.37	52.3	4.7	47.5
	2.03	496	11.7	57.0	5.1	51.8		2.03	529	16.3	57.0	5.1	51.9
	2.29	504	24.3	61.9	5.5	56.3		2.29	534	36.1	61.9	5.5	56.4
	2.54	508	50.4	67.1	5.9	61.2		2.54	536	79.9	67.1	5.9	61.2
	2.79	509	105	72.8	6.3	66.5		2.67	537	119	69.9	6.1	63.8
	3.00	510	188	78.0	6.6	71.4		2.74	537	151	71.6	6.2	65.4
36	0.87	0	0.410×10 ⁻³	34.9×10 ³	3.2×10 ³	31.7×10 ³	40	0.86	0	0.456×10 ⁻³	34.7×10 ³	3.2×10 ³	31.5×10 ³
	1.02	104	.637	38.0	3.5	34.5		1.02	86	.764	38.0	3.5	34.5
	1.27	210	1.35	42.9	3.9	39.0		1.27	199	1.76	42.9	3.9	39.0
	1.52	277	2.86	47.6	4.4	43.3		1.52	255	4.05	47.6	4.3	43.3
	1.78	312	6.04	52.3	4.7	47.5		1.78	277	9.34	52.3	4.7	47.5
	2.03	329	12.8	57.0	5.1	51.9		2.03	284	21.5	57.0	5.1	51.8
	2.29	337	27.1	61.9	5.5	56.4		2.16	287	32.6	59.4	5.3	54.1
	2.54	340	57.3	67.1	5.9	61.2		2.29	289	49.5	61.8	5.5	56.3
	2.67	341	83.4	69.9	6.1	63.8		2.41	290	75.2	64.4	5.7	58.7
	2.79	342	121	72.8	6.3	66.6		2.64	291	159	69.3	6.0	63.2

TABLE II. - Continued. CRACK GROWTH DATA FOR 2014-T6 ALUMINUM AT -320° F (77 K)

(b) Continued. SI Units

Specimen	Crack length, 2a, cm	Number of load cycles, N	Crack growth rate, da/dN, cm/cycle	Stress intensity factor, K, MN/m ^{3/2}		Change in stress intensity factor, ΔK	Specimen	Crack length, 2a, cm	Number of load cycles, N	Crack growth rate, da/dN, cm/cycle	Stress intensity factor, K, MN/m ^{3/2}		Change in stress intensity factor, ΔK
				Maximum	Minimum						Maximum	Minimum	
				41	0.89 1.02 1.27 1.52 1.78 2.03 2.29 2.41 2.54 2.82	0 49 147 192 209 217 220 221 222 223					0.675×10 ⁻³ .992 2.14 4.62 9.97 21.5 46.4 68.2 100 233	35.5×10 ³ 38.1 43.0 47.7 52.4 57.1 62.0 64.5 67.2 73.6	3.3×10 ³ 3.5 3.9 4.4 4.7 5.1 5.5 5.7 5.9 6.3
42	0.91 1.02 1.27 1.52 1.78 2.03 2.16 2.29 2.41 2.62	0 39 161 232 260 280 284 288 290 291	0.371×10 ⁻³ .516 1.18 2.69 6.15 14.1 21.3 32.1 48.6 94.0	35.9×10 ³ 38.0 42.9 47.6 52.3 57.0 59.4 61.8 64.4 68.7	3.3×10 ³ 3.5 3.9 4.4 4.7 5.1 5.3 5.5 5.7 6.0	32.6×10 ³ 34.5 39.0 43.3 47.5 51.8 54.0 56.3 58.7 62.7	46	0.94 1.02 1.52 2.03 2.29 2.54 2.79 3.05 3.43 3.66	0 233 726 884 913 930 938 942 944 945	0.218×10 ⁻³ .264 .958 3.47 6.61 12.6 24.0 45.6 120 214	28.3×10 ³ 29.5 36.8 43.7 47.2 50.8 54.7 58.8 65.8 70.9	2.7×10 ³ 2.8 3.5 4.1 4.4 4.7 5.0 5.3 5.8 6.2	25.6×10 ³ 26.7 33.3 39.6 42.8 46.1 49.6 53.4 60.0 64.7
43	0.82 .89 1.02 1.14 1.27 1.52 1.78 1.90 2.16 2.39	0 41 92 131 145 162 171 173 174 175	0.907×10 ⁻³ 1.16 1.80 2.82 4.41 10.8 26.3 41.1 100 224	33.9×10 ³ 35.4 38.0 40.5 42.9 47.6 52.2 54.6 59.3 63.9	3.1×10 ³ 3.3 3.5 3.7 3.9 4.4 4.7 4.9 5.3 5.7	30.8×10 ³ 32.1 34.5 36.8 39.0 43.3 47.5 49.6 54.0 58.2	47	0.87 1.14 1.52 1.90 2.29 2.67 2.92 3.18 3.43 3.63	0 737 1131 1279 1337 1363 1375 1379 1380 1381	0.148×10 ⁻³ .296 .764 1.97 5.10 13.2 24.8 46.7 87.9 146	27.1×10 ³ 31.3 36.7 41.9 47.1 52.6 56.6 60.9 65.7 70.2	2.6×10 ³ 3.0 3.5 3.9 4.4 4.9 5.2 5.5 5.8 6.1	24.5×10 ³ 28.4 33.3 38.0 42.7 47.8 51.4 55.4 59.9 64.0
44	0.87 1.02 1.27 1.52 1.78 2.03 2.16 2.29 2.41 2.59	0 86 184 229 247 255 258 259 261 262	0.550×10 ⁻³ .884 1.98 4.43 9.92 22.2 33.2 49.7 74.4 131	34.9×10 ³ 38.0 42.9 47.6 52.2 56.9 59.3 61.8 64.4 68.1	3.2×10 ³ 3.5 3.9 4.4 4.7 5.1 5.3 5.5 5.7 6.0	31.7×10 ³ 34.5 39.0 43.3 47.5 51.8 54.0 56.3 58.7 62.2	48	0.92 1.02 1.27 1.52 2.03 2.54 2.79 3.05 3.30 3.45	0 227 716 880 1101 1155 1167 1174 1177 1178	0.151×10 ⁻³ .193 .369 .708 2.60 9.55 18.3 35.1 67.2 99.3	27.9×10 ³ 29.4 33.2 36.8 43.7 50.8 54.6 58.7 63.2 66.3	2.7×10 ³ 2.8 3.2 3.5 4.1 4.7 5.0 5.3 5.7 5.9	25.3×10 ³ 26.6 30.0 33.3 39.6 46.0 49.6 53.3 57.6 60.4

TABLE II. - Concluded. CRACK GROWTH DATA FOR 2014-T6 ALUMINUM AT -320° F (77 K)

(b) Concluded. SI Units

Specimen	Crack length, 2a, cm	Number of load cycles, N	Crack growth rate, da/dN, cm/cycle	Stress intensity factor, K, MN/m ^{3/2}		Change in stress intensity factor, ΔK	Specimen	Crack length, 2a, cm	Number of load cycles, N	Crack growth rate, da/dN, cm/cycle	Stress intensity factor, K, MN/m ^{3/2}		Change in stress intensity factor, ΔK
				Maximum	Minimum						Maximum	Minimum	
				49	0.88 1.27 1.78 2.29 2.54 2.79 3.05 3.30 3.56 3.76						0 966 1340 1476 1519 1539 1550 1555 1558 1559	0.125×10 ⁻³ .311 1.01 3.30 5.96 10.7 19.4 35.0 63.2 101	
50	0.87 1.02 1.27 1.52 1.78 2.03 2.29 2.67 3.05 3.40	0 525 870 1033 1156 1231 1275 1303 1312 1314	0.120×10 ⁻³ .176 .349 .693 1.38 2.73 5.43 15.2 42.5 111	27.2×10 ³ 29.5 33.2 36.8 40.2 43.7 47.2 52.7 58.7 65.3	2.6×10 ³ 2.8 3.2 3.5 3.8 4.1 4.4 4.9 5.3 5.8	24.6×10 ³ 26.7 30.1 33.3 36.4 39.6 42.8 47.8 53.4 59.5	53	0.91 1.27 1.65 1.90 2.16 2.41 2.67 2.92 3.18 3.43	0 662 840 899 931 948 956 962 964 965	0.228×10 ⁻³ .585 1.57 3.03 5.86 11.3 21.9 42.2 81.6 158	27.7×10 ³ 33.2 38.5 42.5 45.4 49.0 52.7 56.6 60.9 65.8	2.6×10 ³ 3.2 3.6 3.9 4.3 4.6 4.9 5.2 5.5 5.8	25.1×10 ³ 30.1 34.9 38.0 41.2 44.4 47.8 51.4 55.4 59.9
51	0.96 1.14 1.52 1.90 2.29 2.54 2.79 3.05 3.30 3.48	0 441 971 1148 1235 1261 1283 1290 1294 1295	0.127×10 ⁻³ .203 .543 1.45 3.88 7.48 14.4 27.7 53.5 84.6	28.6×10 ³ 31.4 36.8 42.0 47.2 50.8 54.6 58.7 63.3 66.8	2.7×10 ³ 3.0 3.5 3.9 4.4 4.7 5.0 5.3 5.7 5.9	25.9×10 ³ 28.4 33.3 38.0 42.8 46.1 49.6 53.4 57.6 60.9	54	0.92 1.27 1.65 2.03 2.29 2.54 2.79 3.05 3.30 3.56	0 726 1031 1174 1223 1248 1269 1273 1275 1276	0.119×10 ⁻³ .301 .820 2.24 4.36 8.52 16.6 32.4 63.3 124	27.9×10 ³ 33.2 38.5 43.7 47.2 50.8 54.6 58.7 63.3 68.5	2.7×10 ³ 3.2 3.6 4.1 4.4 4.7 5.0 5.3 5.7 6.0	25.2×10 ³ 30.1 34.9 39.6 42.8 46.1 49.6 53.4 57.6 62.5

TABLE III. - INITIAL CONDITIONS AND TEST DATA FOR R_1 RATIO EFFECTS FOR 2014-T6 ALUMINUM AT -320°F (77K)

(a) U. S. Customary Units

Specimen	Frequency, f , Hz	Crack length, in.		Gross fracture stress, σ_f , ksi		Initial stress intensity, K , ksi $\sqrt{\text{in.}}$		Ratio of $K_{\text{min}}/K_{\text{max}}$, R_1	Initial stress intensity factor range, ΔK_I , ksi $\sqrt{\text{in.}}$	Ratio of maximum initial to critical stress intensity, $K_{\text{max},i}/K_c$	Ratio of maximum initial to nominal critical stress intensity, $K_{\text{max},i}/K_{\text{cn}}$	Maximum stress intensity for last complete cycle before failure, $K_{\text{max},i}$, ksi $\sqrt{\text{in.}}$	Cycles to failure, N_f	Percentage of critical fracture stress, $\% \sigma_c^a$
		Initial, $2a_i$	Last, $2a_f$	Minimum	Maximum	Minimum	Maximum							
1	0.5	0.32	0.85	35.8	47.7	27.1	38.2	0.71	11.1	0.59	0.90	69.3	4016	90
2		.31	.83	35.8	47.7	26.9	37.9	.71	11.0	.59	.89	68.1	4092	
3		.32	.84	23.9	31.1	17.4	38.3	.46	20.8	.59	.90	68.7	404	
4		.31	.97	23.9	31.1	17.0	37.4	.46	20.4	.58	.88	77.8	586	
5		.32	.85	11.9	23.9	8.5	38.1	.22	29.6	.59	.87	69.3	146	
6		.31	.77	11.9	23.9	8.4	37.7	.22	29.3	.59	.89	64.3	130	
7		.31	.80	0	0	0	37.7	0	37.7	.59	.89	66.2	55	
8		.30	.74	0	0	0	37.2	0	37.2	.58	.88	62.6	69	
9	0.5	0.31	1.05	26.6	39.8	19.3	30.1	0.64	10.9	0.47	0.71	63.6	5990	75
10		.30	1.08	26.6	39.8	19.1	39.9	.64	10.8	.46	.71	65.1	8617	
11		.31	1.09	19.9	31.1	14.3	30.4	.47	16.1	.47	.71	65.7	1748	
12		.33	1.13	19.9	31.1	14.6	31.1	.47	16.4	.48	.73	68.0	1509	
13		.30	1.11	19.9	31.1	14.1	29.9	.47	15.9	.47	.71	66.9	2169	
14		.31	1.04	9.9	30.2	7.0	30.2	.23	23.2	.47	.71	63.0	560	
15		.30	1.05	9.9	29.9	6.9	29.9	.23	23.0	.47	.71	63.5	777	
16		.32	.98	0	0	0	30.6	0	30.6	.48	.72	60.0	208	
17		.30	1.02	0	0	0	29.8	0	29.8	.46	.70	62.0	248	
18	0.5	0.31	1.37	15.9	31.8	11.2	23.3	0.48	12.1	0.36	0.55	60.8	7313	60
19		.31	1.50	15.9	31.8	11.4	23.6	.48	12.2	.37	.55	68.0	6985	
20		.32	1.37	8.0	31.1	5.7	23.8	.24	18.1	.37	.56	60.8	1986	
21		.30	1.33	8.0	31.1	5.5	23.1	.24	17.6	.36	.55	59.0	2303	
22		.32	1.48	8.0	31.1	5.7	23.7	.24	18.0	.37	.56	66.8	1968	
23		.32	1.28	0	0	0	23.7	0	23.7	.37	.56	56.7	1317	
24		.32	1.38	0	0	0	23.7	0	23.7	.37	.56	61.4	1067	

^a $\sigma_c = 53.0$ ksi (gross failure stress for cracked specimen in fig. 1).

(b) SI Units

Specimen	Frequency, f , Hz	Crack length, cm		Gross fracture stress, σ , MN/cm ²		Initial stress intensity, K , MN/m ^{3/2}		Ratio of K_{min}/K_{max} , R_i	Initial stress intensity factor range, ΔK_i , MN/m ^{3/2}	Ratio of maximum initial to critical stress intensity, $K_{max,i}/K_c$	Ratio of maximum initial to nominal critical stress intensity, $K_{max,i}/K_{cn}$	Maximum stress intensity for last complete cycle before failure, $K_{max,i}$, MN/m ^{3/2}	Cycles to failure, N_f	Percentage of critical fracture stress, $\% \sigma_c$
		Initial, $2a_i$	Last, $2a_L$	Minimum	Maximum	Minimum	Maximum							
1	0.5	0.81	2.15	24.7	32.9	29.8	42.0	0.71	12.2	0.59	0.90	76.2	4016	90
2		.80	2.11	24.7	41.7	29.6	41.7	.71	12.1	.59	.89	74.8	4092	
3		.81	2.13	16.5	42.0	19.1	42.0	.46	22.9	.59	.90	75.5	404	
4		.79	2.54	16.5	41.5	18.9	41.5	.46	22.6	.58	.88	88.2	586	
5		.86	2.16	8.2	43.5	9.7	43.5	.22	33.8	.59	.87	76.2	146	
6		.79	1.96	8.2	41.4	9.3	41.4	.22	32.2	.59	.89	70.7	130	
7		.78	2.03	0	41.4	0	41.4	0	41.4	.59	.89	72.8	55	
8		.77	1.88	0	40.9	0	40.9	0	40.9	.58	.88	68.8	69	
9	0.5	0.78	2.67	18.4	27.5	21.2	33.1	0.64	11.9	0.47	0.71	69.9	5990	75
10		.77	2.74	18.4	32.9	21.0	32.9	.64	11.8	.47	.71	71.6	8617	
11		.80	2.77	13.7	33.4	15.7	33.4	.47	17.6	.47	.71	72.2	1748	
12		.83	2.87	13.7	34.1	16.1	34.1	.47	18.1	.48	.73	74.7	1509	
13		.77	2.82	13.7	32.9	15.5	32.9	.47	17.4	.47	.71	73.5	2169	
14		.79	2.64	6.8	33.2	7.7	33.2	.23	25.5	.47	.71	69.2	560	
15		.77	2.67	6.8	32.9	7.6	32.9	.23	25.2	.47	.71	69.8	777	
16		.81	2.49	0	33.6	0	33.6	0	33.6	.48	.72	66.0	208	
17		.77	2.59	0	32.8	0	32.8	0	32.8	.46	.70	68.2	248	
18	0.5	0.77	3.48	11.0	21.9	12.3	25.6	0.48	13.2	0.36	0.55	66.8	7313	60
19		.80	3.81	11.0	25.9	12.5	25.9	.48	13.4	.37	.55	74.7	6985	
20		.81	3.48	5.5	26.1	6.2	26.1	.24	19.9	.37	.56	66.8	1986	
21		.76	3.38	5.5	25.4	6.1	25.4	.24	19.3	.36	.55	64.8	2303	
22		.80	3.76	5.5	26.1	6.2	26.1	.24	19.8	.37	.56	73.5	1968	
23		.80	3.25	0	26.0	0	26.0	0	26.0	.37	.56	62.3	1317	
24		.81	3.51	0	26.1	0	26.1	0	26.1	.37	.56	67.4	1067	

 $b \sigma_c = 36.6 \text{ MN/cm}^2$

TABLE IV. - INITIAL CONDITIONS AND TEST DATA FOR CYCLIC RATE AND SCATTER EFFECTS FOR 2014-T6 ALUMINUM AT -320° F (77 K)

(a) U. S. Customary Units

Specimen	Frequency, f , Hz	Crack length, in.		Gross fracture stress, σ_f , ksi		Initial stress intensity, K		Ratio of K_{min}/K_{max} , R_i	Initial stress intensity factor range, ΔK_i , ksi $\sqrt{\text{in.}}$	Ratio of maximum initial to critical stress intensity, $K_{max,i}/K_c$	Ratio of maximum initial to nominal critical stress intensity, $K_{max,i}/K_{cn}$	Maximum stress intensity for last complete cycle before failure, $K_{max,l}$, ksi $\sqrt{\text{in.}}$	Cycles to failure, N_f	Percentage of critical fracture stress, $\% \sigma_c^a$
		Initial, $2a_i$	Last, $2a_f$	Minimum	Maximum	Minimum	Maximum							
25	0.5	0.29	0.79	4.8	47.7	3.2	36.5	0.09	33.2	0.57	0.86	65.5	97	90
26	→	.32	.73	→	→	3.4	38.1	→	34.7	.59	.89	62.0	65	→
27	→	.34	.74	→	→	3.5	39.6	→	36.1	.62	.92	62.6	52	→
28	→	.34	.74	→	→	3.5	39.6	→	36.0	.62	.92	62.6	56	→
29	→	.35	.81	→	→	3.5	39.9	→	36.4	.62	.93	66.8	44	→
30	0.05	0.39	0.75	4.8	47.7	3.8	42.4	0.09	38.6	0.66	0.98	63.2	20	90
31	→	.34	.75	→	→	3.5	39.8	→	36.2	.62	.93	63.2	25	→
32	→	.33	.76	→	→	3.5	39.0	→	35.5	.61	.91	63.8	33	→
33	→	.32	.76	→	→	3.4	38.5	→	35.1	.60	.90	63.8	39	→
34	→	.35	.76	→	→	3.6	40.1	→	36.5	.62	.93	63.8	31	→
35	0.5	0.32	1.18	4.0	39.8	2.9	30.8	0.09	27.8	0.48	0.72	71.0	510	75
36	→	.34	1.10	→	→	2.9	31.8	→	28.8	.49	.74	66.3	342	→
37	→	.30	1.13	→	→	2.7	29.7	→	27.0	.46	.70	68.0	490	→
38	→	.31	1.14	→	→	2.8	30.3	→	27.5	.47	.71	68.6	516	→
39	→	.30	1.08	→	→	2.7	29.5	→	26.7	.46	.69	65.2	537	→
40	0.05	0.34	1.04	4.0	39.8	2.9	31.6	0.09	28.7	0.49	0.74	63.0	291	75
41	→	.35	1.11	→	→	3.0	32.3	→	29.3	.50	.75	70.0	223	→
42	→	.36	1.03	→	→	3.0	32.7	→	29.7	.51	.76	62.5	291	→
43	→	.32	.94	→	→	2.9	30.9	→	28.0	.48	.72	58.1	175	→
44	→	.34	1.02	→	→	2.9	31.8	→	28.8	.49	.74	62.0	262	→
45	0.5	0.34	1.39	3.2	31.8	2.3	24.5	0.10	22.2	0.38	0.57	61.8	1478	60
46	→	.37	1.44	→	→	2.5	25.8	→	23.3	.40	.60	64.5	945	→
47	→	.34	1.43	→	→	2.3	24.6	→	22.3	.38	.57	63.9	1381	→
48	→	.36	1.41	→	→	2.4	25.4	→	23.0	.40	.59	66.3	1178	→
49	→	.35	1.48	→	→	2.4	24.8	→	22.5	.39	.58	66.8	1559	→
50	0.05	0.34	1.34	3.2	31.8	2.4	24.8	0.10	22.4	0.39	0.58	59.4	1314	60
51	→	.38	1.37	→	→	2.5	26.1	→	23.6	.41	.60	60.8	1295	→
52	→	.35	1.35	→	→	2.4	25.1	→	22.7	.39	.58	59.9	1346	→
53	→	.36	1.35	→	→	2.4	25.3	→	22.8	.39	.59	59.9	965	→
54	→	.36	1.40	→	→	2.4	25.4	→	23.0	.39	.59	62.3	1276	→

^a $\sigma_c = 53.0$ ksi.

(b) SI Units

Specimen	Frequency, f , Hz	Crack length, cm		Gross fracture stress, σ , MN/cm ²		Initial stress intensity, K , 3/2 MN/m ^{3/2}		Ratio of K_{min}/K_{max} , R_i	Initial stress intensity factor range, ΔK_i , MN/m ^{3/2}	Ratio of maximum initial to critical stress intensity, $K_{max,i}/K_c$	Ratio of maximum initial to nominal critical stress intensity, $K_{max,i}/K_{cn}$	Maximum stress intensity for last complete cycle before failure, $K_{max,i}^l$, MN/m ^{3/2}	Cycles to failure, N_f	Percentage of critical fracture stress, $\% \sigma_c^b$
		Initial, $2a_i$	Last, $2a_f$	Minimum	Maximum	Minimum	Maximum							
25	0.5	0.74	2.01	3.3	32.9	3.6	40.1	0.09	36.5	0.57	0.86	72.0	97	90
26		.80	1.85			3.7	41.9		38.2	.59	.89	68.1	65	
27		.86	1.88			3.9	43.5		39.6	.62	.92	68.8	52	
28		.86	1.88			3.9	43.5		39.6	.62	.92	68.7	56	
29		.88	2.06			3.9	43.9		40.0	.62	.93	73.4	44	
30	0.05	0.98	1.90	3.3	32.9	4.1	46.5	0.09	42.4	0.66	0.98	69.4	20	90
31		.87	1.90			3.9	43.7		39.8	.62	.93	69.4	25	
32		.84	1.93			3.8	42.9		39.1	.61	.91	70.1	33	
33		.82	1.93			3.8	42.4		38.6	.60	.90	70.1	39	
34		.88	1.93			3.9	44.0		40.1	.62	.93	70.1	31	
35	0.5	0.82	3.00	2.8	27.5	3.1	33.9	0.09	30.7	0.48	0.72	78.0	510	75
36		.87	2.79			3.2	34.9		31.7	.49	.74	72.8	342	
37		.76	2.87			3.0	32.7		29.6	.46	.70	74.7	490	
38		.79	2.90			3.1	33.3		30.3	.47	.71	75.4	516	
39		.75	2.74			3.0	32.4		29.4	.46	.69	71.6	537	
40	0.05	0.86	2.64	2.8	27.5	3.2	34.7	0.09	31.5	0.49	0.74	69.3	291	75
41		.89	2.82			3.3	35.5		32.2	.50	.75	73.6	223	
42		.91	2.62			3.3	35.9		32.6	.51	.76	68.7	291	
43		.82	2.39			3.1	33.9		30.8	.48	.72	63.9	175	
44		.87	2.59			3.2	34.9		31.7	.49	.74	68.1	262	
45	0.5	0.86	3.53	2.2	21.9	2.6	27.0	0.10	24.4	0.38	0.57	68.0	1478	60
46		.94	3.66			2.7	28.3		25.6	.40	.60	70.9	945	
47		.87	3.63			2.6	27.1		24.5	.38	.57	70.2	1381	
48		.92	3.45			2.7	27.9		25.3	.40	.59	66.3	1178	
49		.88	3.76			2.6	27.3		24.7	.39	.58	73.4	1559	
50	0.05	0.87	3.40	2.2	21.9	2.6	27.2	0.10	24.6	0.39	0.58	65.3	1314	60
51		.96	2.48			2.7	28.6		25.9	.41	.60	66.8	1295	
52		.90	3.43			2.6	27.6		25.0	.39	.58	65.8	1346	
53		.91	3.43			2.6	27.7		25.1	.39	.59	65.8	965	
54		.92	3.56			2.7	27.9		25.2	.39	.59	68.5	1276	

 $b_{\sigma_c} = 36.6 \text{ MN/cm}^2$

NATIONAL AERONAUTICS AND SPACE ADMINISTRATION
WASHINGTON, D. C. 20546
OFFICIAL BUSINESS

FIRST CLASS MAIL

POSTAGE AND FEES PAID
NATIONAL AERONAUTICS AND
SPACE ADMINISTRATION

000 001 57 33 4 8 70046 00076 01100
RESEARCH TRIANGLE INSTITUTE
DEPT. 435 - RESEARCH TRIANGLE CENTER
CAMPUS LABORATORY BLDG
305 KING AVENUE
COLUMBUS, OHIO 43201
ATTN: ROGER J. ROLOFF

POSTMASTER: If Undeliverable (Section 158
Postal Manual) Do Not Return

"The aeronautical and space activities of the United States shall be conducted so as to contribute . . . to the expansion of human knowledge of phenomena in the atmosphere and space. The Administration shall provide for the widest practicable and appropriate dissemination of information concerning its activities and the results thereof."

— NATIONAL AERONAUTICS AND SPACE ACT OF 1958

NASA SCIENTIFIC AND TECHNICAL PUBLICATIONS

TECHNICAL REPORTS: Scientific and technical information considered important, complete, and a lasting contribution to existing knowledge.

TECHNICAL NOTES: Information less broad in scope but nevertheless of importance as a contribution to existing knowledge.

TECHNICAL MEMORANDUMS: Information receiving limited distribution because of preliminary data, security classification, or other reasons.

CONTRACTOR REPORTS: Scientific and technical information generated under a NASA contract or grant and considered an important contribution to existing knowledge.

TECHNICAL TRANSLATIONS: Information published in a foreign language considered to merit NASA distribution in English.

SPECIAL PUBLICATIONS: Information derived from or of value to NASA activities. Publications include conference proceedings, monographs, data compilations, handbooks, sourcebooks, and special bibliographies.

TECHNOLOGY UTILIZATION PUBLICATIONS: Information on technology used by NASA that may be of particular interest in commercial and other non-aerospace applications. Publications include Tech Briefs, Technology Utilization Reports and Notes, and Technology Surveys.

Details on the availability of these publications may be obtained from:

SCIENTIFIC AND TECHNICAL INFORMATION DIVISION
NATIONAL AERONAUTICS AND SPACE ADMINISTRATION
Washington, D.C. 20546